

# Self-Organizing Systems in Planetary Physics : Harmonic Resonances of Planet and Moon Orbits

Markus J. Aschwanden<sup>1</sup>

<sup>1</sup>) *Lockheed Martin, Solar and Astrophysics Laboratory, Org. A021S, Bldg. 252, 3251 Hanover St., Palo Alto, CA 94304, USA; e-mail: aschwanden@lmsal.com*

## ABSTRACT

The geometric arrangement of planet and moon orbits into a regularly spaced pattern of distances is the result of a self-organizing system. The positive feedback mechanism that operates a self-organizing system is accomplished by harmonic orbit resonances, leading to long-term stable planet and moon orbits in solar or stellar systems. The distance pattern of planets was originally described by the empirical Titius-Bode law, and by a generalized version with a constant geometric progression factor (corresponding to logarithmic spacing). We find that the orbital periods  $T_i$  and planet distances  $R_i$  from the Sun are not consistent with logarithmic spacing, but rather follow the quantized scaling  $(R_{i+1}/R_i) = (T_{i+1}/T_i)^{2/3} = (H_{i+1}/H_i)^{2/3}$ , where the harmonic ratios are given by five dominant resonances, namely  $(H_{i+1} : H_i) = (3 : 2), (5 : 3), (2 : 1), (5 : 2), (3 : 1)$ . We find that the orbital period ratios tend to follow the quantized harmonic ratios in increasing order. We apply this harmonic orbit resonance model to the planets and moons in our solar system, and to the exo-planets of 55 Cnc and HD 10180 planetary systems. The model allows us a prediction of missing planets in each planetary system, based on the quasi-regular self-organizing pattern of harmonic orbit resonance zones. We predict 7 (and 4) missing exo-planets around the star 55 Cnc (and HD 10180). The accuracy of the predicted planet and moon distances amounts to a few percents. All analyzed systems are found to have  $\approx 10$  resonant zones that can be occupied with planets (or moons) in long-term stable orbits.

*Subject headings:* planetary systems — planets and satellites: general — stars: individual

## 1. INTRODUCTION

Johannes Kepler was the first to study the distances of the planets to the Sun and found that the inner radii of regular geometric bodies (Platon’s polyhedra solids) approximately match the observations, which he published in his famous *Mysterium Cosmographicum* in 1596. An improved empirical law was discovered by J.B. Titius in 1766, and it was made prominent by Johann Elert Bode (published in 1772), known since then as the *Titius-Bode law*:

$$R_n = \begin{cases} 0.4 & \text{for } n = 1 \\ 0.3 \times 2^{n-2} + 0.4 & \text{for } n = 2, \dots, 10 \end{cases} \quad (1)$$

Only the six planets from Mercury to Saturn were known at that time. The asteroid belt, represented by the largest asteroid body *Ceres* (discovered in 1801), part of the so-called “missing planet” (Jenkins 1878; Napier et al. 1973; Opik 1978), was predicted from the Titius-Bode law, as well as the outer planets Uranus, Neptune, and Pluto, discovered in 1781, 1846, and 1930, respectively. Historical reviews of the Titius-Bode law can be found in Jaki (1972a,b), Ovenden (1972, 1975), Nieto (1972), Chapman (2001a,b), and McFadden et al. (1999, 2007).

Noting early on that the original Titius-Bode law breaks down for the most extremal planets (Mercury at the inner side, and Neptune and Pluto at the outer side), numerous modifications were proposed: such as a 4-parameter polynomial (Blagg 1913; Brodetsky 1914); the Schrödinger-Bohr atomic model with a scaling of  $R_n \propto n(n + 1)$ , where the quantum-mechanical number  $n$  is substituted by the planet number (Wylie 1931; Louise 1982; Scardigli 2007a,b); a geometric progression by a constant factor (Blagg 1913; Nieto 1970; Dermott 1968, 1973; Armellini 1921; Munini and Armellini 1978; Badolati 1982; Rawal 1986, 1989; see compilation in Table 1); fitting an exponential distance law (Pletser 1986, 1988); the introduction of additional planets (Basano and Hughes 1979), applying a symmetry correction to the Jupiter-Sun system (Ragnarsson 1995); tests of random statistics (Dole 1970; Lecar 1973; Dworak and Kopacz 1997; Hayes and Tremaine 1998; Lynch 2003; Neslusan 2004; Cresson 2011; Pletser 2017); self-organization of atomic patterns (Prisniakov 2001), standing waves in the solar system formation (Smirnov 2015), or the Four Poisson-Laplace theory of gravitation (Nyambuya 2015).

Also the significance of the Titius-Bode law for predicting the orbit radii of moons around Jupiter or Saturn was recognized early on (Blagg 1913; Brodetsky 1914; Wylie 1931; Miller 1938a,b; Todd 1938; Cutteridge 1962; Fairall 1963; Dermott 1968; Nieto 1970; Rawal 1978; Hu and Chen 1987), or the prediction of a trans-Neptunian planet “Eris” (Ortiz et al. 2007; Flores-Gutierrez and Garcia-Guerra 2011; Gomes et al. 2016), while more recent usage of the Titius-Bode law is made to predict the distances of exo-planets to their central star (Cuntz 2012; Bovaird and Lineweaver 2013, Bovaird et al. 2015; Poveda and Lara 2008; Lovis et al. 2011; Qian et al. 2011; Huang and Bakos 2014), or a planetary system around a pulsar (Bisnovatyi-Kogan 1993).

Physical interpretations of the Titius-Bode Law involve the accumulation of planetesimals, rather than the creation of enormous proto-planets and proto-satellites (Dai 1975, 1978). N-body (Monte-Carlo-type) computer simulations of the formation of planetary systems were performed, which could reproduce the regular orbital spacings of the Titius-Bode law to some extent (Dole 1970; Lecar 1973; Isaacman and Sagan 1977; Prentice 1977; Estberg and Sheehan 1994), or not (Cameron 1973). Some theories concerning the Titius-Bode law involve orbital resonances in planetary system formation, starting with an early-formed Jupiter which produces a runaway growth of planetary embryos by a cascade of harmonic resonances between their orbits (e.g., Goldreich 1965; Dermott 1968; Tobett et al. 1982; Patterson 1987; Filippov 1991). Alternative models involve the self-gravitational instability in very thin Keplerian disks (Ruediger and Tschaeppe 1988; Rica 1995), the principle of least action interaction (Ovenden 1972; Patton 1988), or scale-invariance of the disk that produces planets (Graner and Dubrulle 1994; Dubrulle and Graner 1994). Analytical models of the Titius-Bode law have been developed in terms of hydrodynamics in thin disks that form rings (Nowotny 1979; Hu and Chen 1987), periodic functions with Tschebischeff polynomials (Dobo 1981), power series expansion (Bass and Popolo 2005), and the dependence of the regularity parameter on the central body mass (Georgiev 2016).

The previous summary reflects the fact that we still do not have a physical model that explains the empirical Titius-Bode law, nor do we have an established quantitative physical model that predicts the exact geometric pattern of the planet distances to the central star, which could be used for searches of exo-solar planets or for missing moons around planets. In this Paper we investigate a physical model that quantitatively explains the distances of the planets from the Sun, based on the most relevant harmonic resonances in planet orbits, which provides a more accurate prediction of planet distances than the empirical Titius-Bode law, or its generalized version with a constant geometric progression factor. This model appears to be universally applicable, to the planets of our solar system, planetary moon systems, Saturn-like ring systems, and stellar exo-planetary systems.

A novel approach of this study is the interpretation of harmonic orbit resonances in terms of a self-organization system (not to be confused with self-organized criticality systems, Bak et al. 1987; Aschwanden et al. 2016). The principle of self-organization is a mechanism that creates spontaneous order out of initial chaos, in contrast to random processes that are governed by entropy. A self-organizing mechanism is spontaneously triggered by random fluctuations, is then amplified by a positive feedback mechanism, and produces an ordered structure without any need of an external control agent. The manifestation of a self-organizing mechanism is often a regular geometric pattern with a quasi-periodic structure in space, see various examples in Fig. 1. The underlying physics can involve non-equilibrium processes, magneto-convection, plasma turbulence, superconductivity, phase transitions, or chemical reactions. The concept of self-organization has been applied to solid state physics and material science (Müller and Parisi 2015), laboratory plasma physics (Yamada 2007, 2010; Zweibel and Yamada 2009); chemistry (Lehn 2002), sociology (Leydesdorff 1993), cybernetics and learning algorithms (Kohonen 1984; Geach 2012), or biology (Camazine et al. 2001). In astrophysics, self-organization has been applied to galaxy and star formation (Bodifée 1986; Cen 2014), astrophysical shocks (Malkov et al. 2000), accretion discs (Kunz and Lesur 2013), magnetic reconnection (Yamada 2007, 2010; Zweibel and Yamada 2009); turbulence (Hasegawa 1985), magneto-hydrodynamics (Horiuchi and Sato 1985); planetary atmosphere physics (Marcus 1993); magnetospheric physics (Valdivia et al. 2003; Yoshida et al. 2010), ionospheric physics (Leyser 2001), solar magneto-convection (Krishan 1991; Kitiashvili et al. 2010), and solar corona physics (Georgoulis 2005; Uzdensky 2007). Here we apply the concept of self-organization to the solar system, planetary moon systems, and exo-planet systems, based on the physical mechanism of harmonic orbit resonances.

The plan of the paper is an analytical derivation of the harmonic orbit resonance model (Section 2), an application to observed data of our solar system planets, the moon systems of Jupiter, Saturn, Uranus, and Neptune, and two exo-planet systems (Section 3), a discussion in the context of previous work (Section 4), and final conclusions (Section 5).

## 2. THEORY

### 2.1. The Titius-Bode Law

Kepler’s third law can directly be derived from the equivalence of the kinetic energy of a planet,  $E_{kin} = (1/2)m_P v^2$ , with the gravitational potential energy,  $E_{pot} = \Gamma M_\odot m_P / R$ , which yields the scaling between the mean planet velocity  $v$  and the distance  $R$  of the planet from the Sun,

$$v \propto R^{-1/2} , \quad (2)$$

and by using the relationship of the mean velocity,  $v = 2\pi R/T$ , yields

$$R \propto T^{2/3} , \quad (3)$$

which is the familiar third Kepler law, where  $\Gamma$  is the universal gravitational constant,  $m_P$  is the planet mass,  $M_\odot$  the solar mass, and  $T$  is the time period of a planet orbit.

The empirical Titius-Bode law (Eq. 1) tells us that there is a regular spacing between the planet distances  $R$  and the orbital periods  $T$ , which predicts a distance ratio of  $\approx 2$  for subsequent planets  $(n + 1)$  and  $(n)$ , in the asymptotic limit of large distances,  $R \gg 0.4$  AU,

$$\frac{R_{n+1}}{R_n} = \frac{0.3 \times 2^{n-1} + 0.4}{0.3 \times 2^{n-2} + 0.4} \approx 2 . \quad (4)$$

According to Kepler’s third law (Eq. 3), this would imply an orbital period ratio of

$$\frac{T_{n+1}}{T_n} = \left( \frac{R_{n+1}}{R_n} \right)^{3/2} \approx 2^{3/2} \approx 2.83 . \quad (5)$$

Thus, the Titius-Bode law predicts a non-harmonic ratio for the orbital periods, which is in contrast to celestial mechanics models with harmonic resonances (Peale 1976). In the following we will also see that the assumption of a logarithmic spacing in planet distances is incorrect, which explains the failure of the original Titius-Bode law for the most extremal planets in our solar system (Mercury, Neptune, Pluto).

## 2.2. The Generalized Titius-Bode Law

A number of authors modified the Titius-Bode law in terms of a geometric progression with a constant factor  $Q$  between subsequent planet distances, which was called the generalized Titius-Bode law,

$$\frac{R_{n+1}}{R_n} = Q , \quad (6)$$

which reads as

$$R_n = R_3 \times Q^{n-3}, \quad i = 1, \dots, n , \quad (7)$$

if the third planet ( $i = 3$ ), our Earth, is used as the reference distance  $R_3 = 1$  astronomical unit (AU). If we apply Kepler’s third law again (Eq. 5), we find an orbital period ratio  $q$  that is related to the distance ratio  $Q$  by  $q = Q^{3/2}$ ,

$$q = \frac{T_{n+1}}{T_n} = \left( \frac{R_{n+1}}{R_n} \right)^{3/2} = Q^{3/2} . \quad (8)$$

Applying this scaling law to the empirical factors  $Q$  found by various authors, we find distance ratios in the range of  $Q = 1.26 - 2.00$  (Table 1, column 1) for geometric progression factors, and  $q = 1.41 - 2.82$  for orbital period ratios (Table 1, column 2). None of those time period ratios matches a low harmonic ratio  $q$ , such as (3:2)=1.5, (2:1)=2, or (3:1)=3. To our knowledge, none of the past studies found a relationship between the empirical Titius-Bode law and harmonic periods, as it would be expected from the viewpoint of harmonic resonance interactions in celestial mechanics theory, as applied to orbital resonances in the solar system (Peale 1976), or to the formation of the Cassini division in Saturn’s ring system (Goldreich and Tremaine 1978; Lissauer and Cuzzi 1982). Moreover, the generalized Titius-Bode law assumes logarithmically spaced planet distances, quantified with the constant geometric progression factor  $Q$  (Eq. 6), which turns out to be incorrect for individual planets, but can still be useful as a simple strategy to estimate the location of missing moons and exo-planets (Bovaird and Lineweaver 2013; Bovaird et al. 2015).

## 2.3. Orbital Resonances

Orbital resonances tend to stabilize long-lived orbital systems, such as in our solar system or in planetary moon systems. Computer simulations of planetary systems have demonstrated that injection of planets into circular orbits tend to produce dynamically unstable orbits, unless their orbital periods settle into harmonic ratios, also called commensurabilities (for reviews, see, e.g., Peale 1976; McFadden 2007). For instance, the first three Galilean satellites of Jupiter (Io, Europa, Ganymede) exhibit a resonance (known already to Laplace 1829),

$$\nu_1 - 3\nu_2 + 2\nu_3 \approx 0 , \quad (9)$$

where the frequencies  $\nu_i = 1/T_i$  correspond to the reciprocal orbital periods  $T_i$ , with  $T_1 = 1.769$  days for Io,  $T_2 = 3.551$  days for Europa, and  $T_3 = 7.155$  days for Ganymede), fulfilling the resonance condition (Eq. 9) with an accuracy of order  $\approx 10^{-5}$ , and using more accurate orbital periods even to an accuracy of  $\approx 10^{-9}$  (Peale 1976).

Our goal is to predict the planet distances  $R$  from the Sun based on their most likely harmonic orbital resonances. Some two-body resonances of solar planets are mentioned in the literature, such as the resonances (5:2) for the Jupiter-Saturn system, (2:1) for the Uranus-Neptune system, (3:1) for the Saturn-Uranus system, and (3:2) for the Neptune-Pluto system (e.g., see review of Peale 1976). If we find the most likely resonance between two neighbored planet orbits with periods  $T_i$  and  $T_{i+1}$ , we can apply Kepler’s third law  $R \propto T^{2/3}$  to predict the relative distances  $R_i$  and  $R_{i+1}$  of the planets from the Sun, which allows us also to test the Titius-Bode law as well as the generalized Titius-Bode law.

Orbital resonances in the solar system are all found for small numbers of integers, say for harmonic numbers in the range of  $H=1$  to  $H=5$  (e.g., see Table 1 in Peale 1976). If we consider all possible resonances in this number range, we have nine different harmonic ratios, which includes  $(H_i : H_{i+1}) = (5:4)$ ,  $(4:3)$ ,  $(3:2)$ ,  $(5:3)$ ,  $(2:1)$ ,  $(5:2)$ ,  $(3:1)$ ,  $(4:1)$ ,  $(5:1)$ , sorted by increasing ratios  $q = (H_{i+1}/H_i)$ , as shown in Fig. 2a. The harmonic ratios vary in the range of  $q = [1.2, \dots, 5]$  (Fig. 2a). The related planet distance ratios  $Q$  can be obtained from Kepler’s third law, which produces ratios of  $Q = q^{2/3}$  (Eq. 8), which yields a range of  $Q = [1.129, \dots, 2.924]$  (Fig. 2b). This defines possible distance ratios  $Q = R_{i+1}/R_i$  between neighbored planets varying by a factor of three, which is clearly not consistent with a single constant, as assumed in the generalized Titius-Bode law.

The frequency of strongest gravitational interaction between two neighbored planets is given by the time interval  $t_{conj}$  between two subsequent planet conjunctions, which is defined by the orbital periods  $T_1$  and  $T_2$  as

$$\frac{1}{t_{conj}} = \frac{1}{T_1} - \frac{1}{T_2}, \quad \text{for } T_2 > T_1. \quad (10)$$

We see that the conjunction time  $t_{conj}$  approaches infinity in the case of two orbits in close proximity ( $T_2 \gtrsim T_1$ ), while it becomes largest for  $T_2 \gg T_1$ . The conjunction time is plotted as a function of the harmonic ratios in Fig. 2c, which clearly shows that the conjunction times decreases (Fig. 2c) with increasing harmonic ratios (Fig. 2a). Since the gravitational force decreases with the square of the distance  $\Delta R = (R_2 - R_1)$ , i.e.,  $F_{grav} \propto m_1 m_2 / \Delta R^2$ , neighbored planet pairs matter more for gravitational interactions, such as for stabilizing resonant orbits, than remote planets. On the other side, if the planets are too closely spaced, they have similar orbital periods and the conjunction times increases, which lowers the chance for gravitational stabilization interactions. So, there is a trade-off between these two competing effects that determines which relative distance is at optimum for maintaining stable long-lived orbits. We will see in the following that the “sweet spot” occurs for harmonic ratios between  $q = 3/2 = 1.5$  and  $q = 3/1 = 3.0$ , a range that includes only five harmonic ratios, namely (3:2), (5:3), (2:1), (5:2), (3:1), which are marked with hatched areas in Fig. 2.

#### 2.4. The Harmonic Orbit Resonance Model

We investigate now a quantitative model that can fit the distances of the planets from the Sun, which we call the harmonic orbit resonance model. The basic assumption in our model is that a two-body resonance exists between two neighbored planets in stable long-term orbits, which can be defined by the resonance

condition (similar to Eq. 9),

$$(H_i \nu_i - H_{i+1} \nu_{i+1}) \propto \omega_{i,i+1} , \quad (11)$$

where  $H_i$  and  $H_{i+1}$  are the (small) integer numbers of a harmonic ratio  $q_{i,i+1} = (H_{i+1}/H_i)$ , and  $\nu_1$  and  $\nu_2$  are the frequencies of the orbital periods,  $\nu_i = 1/T_i$ , which can be expressed as,

$$1 - \frac{H_{i+1}}{H_i} \left( \frac{T_i}{T_{i+1}} \right) = \omega_{i,i+1} , \quad (12)$$

where  $\omega_{i,i+1}$  is the residual that remains from unaccounted resonances from possible third or more bodies involved in the resonance. The normalization by the factor  $H_i \nu_i$  in (Eq. 11) serves the purpose to make the residual values compatible for different planet pairs.

In order to find the harmonic ratios  $H_{i+1} : H_i$  that fulfill the resonance condition (Eq. 12), we have to insert the orbital time periods  $T_i, T_{i+1}$  into Eq. (12) and find the best-fitting harmonic ratios that yield a minimum in the absolute value of the resulting residual  $|\omega_{i,i+1}|$ . This procedure is illustrated in Fig. 3 for the 9 neighbored planet pair systems, where we included all 9 cases of different harmonic ratios ( $H_i : H_{i+1}$ ) = (5:4), (4:3), (3:2), (5:3), (2:1), (5:2), (3:1), (4:1), (5:1), sorted in rank number on the x-axis, while the residual value is plotted on the y-axis. We see (in Fig. 3) that we find solutions with a residual value in the range of  $\omega_{i,i+1} \approx 0.005 - 0.06$  in each case. The result for the 9 planet pairs shown in Fig. 3 confirms that the best-fit resonances are confined to the small range of 5 cases between  $q = 3/2 = 1.5$  and  $q = 3/1 = 3.0$ , namely (3:2), (5:3), (2:1), (5:2), (3:1), as marked in Fig. 2. Thus, the result of the harmonic orbit resonance model for our solar system (based on the smallest two-body residuals  $\omega_{min}$ , Fig. 3), are the harmonic orbit resonances of (3:2) for Neptune-Pluto, (5:3) for Venus-Earth, (5:2) for Mercury-Venus, Mars-Ceres, Ceres-Jupiter, Jupiter-Saturn, (2:1) for Earth-Mars, Uranus-Neptune, and (3:1) for Saturn-Uranus (Fig. 3), which agree with all previously cited results (e.g., see review of Peale 1976).

We investigated also the role of Jupiter, the most massive planet, in the three-body resonance condition (by expanding Eq. 12),

$$1 - \frac{H_{i+1}}{H_i} \left( \frac{T_i}{T_{i+1}} \right) - \frac{H_{Jup}}{H_i} \left( \frac{T_i}{T_{Jup}} \right) = \omega_{i,i+1} , \quad (13)$$

but found identical results (yielding  $H_{Jup} = 0$ ), except for the three-body configuration of Ceres-Mars-Jupiter, where an optimum harmonic ratio of (2:1) was found, instead of (5:3), for two-body systems. From this we conclude that the two-body interactions of neighbored planet-planet systems are more important in the resonant stabilization of orbits than the influence of the largest giant planet (Jupiter), except for planet-asteroid pairs.

Once we know the harmonic ratio for each pair of neighbored planets, we can apply Kepler's third law to the orbital periods  $T_i$  and predict the distances  $R_i$  of the planets,

$$\left( \frac{R_{i+1}}{R_i} \right) = \left( \frac{T_{i+1}}{T_i} \right)^{2/3} = \left( \frac{H_{i+1}}{H_i} \right)^{2/3} . \quad (14)$$

where  $H_i$  and  $H_{i+1}$  are small integer numbers (from 1 to 5) that define the optimized harmonic orbit resonance ratios. Specifically, the five allowed harmonic time period ratios allow only the values  $q_i = H_{i+1}/H_i = 1.5, 1.667, 2.0, 2.5, \text{ and } 3.0$ . Applying Kepler's law, this selection of harmonic time periods yields the 5 discrete distance ratios  $Q_i = q_i^{(2/3)} = [1.31, 1.40, 1.59, 1.84, 2.08]$ . The (arithmetic) averages of these predicted ratios are  $\langle q \rangle = 2.25 \pm 0.75$ ,  $\langle Q \rangle = 1.70 \pm 0.4$ . In the following we will also refer to the extremal values,  $[q_{min}, q_{max}] = [1.5, 3.0]$  and  $[Q_{min}, Q_{max}] = [1.31, 2.08]$ .

This physical model is distinctly different from the empirical Titius-Bode law (Eq. 1), which assumes a constant value  $q_i = 2^{3/2} = 2.83$  (Eq. 4), in the limit of  $R \gg 0.4$  AU, or from its generalized form with an unquantified constant  $Q = q^{2/3}$  (Eq. 6). What is common to all three models is that the planet distances can be defined in an iterative way, e.g.,  $(R_{i+1}/R_i)$ . However, both the original and the generalized Titius-Bode law are empirical relationships, rather than based on a physical model. Moreover, both the original and the generalized Titius-Bode relationships assume a logarithmic spacing of planet distances with a constant geometric progression factor  $Q$ , while the harmonic orbit resonance model predicts 5 quantized values for the planet distance ratios  $Q_i$ .

## 2.5. Fitting the Geometric Progression Factor

So far we discussed three different models to describe the distance pattern of planets to the Sun, which we quantified with the geometric progression factor  $Q_i$ , or time period progression factor  $q_i = Q_i^{3/2}$ , namely (1)  $q_i \approx 2^{3/2}$  for the Titius-Bode law, (2)  $q_i = \text{const}$  for the generalized Titius-Bode law, and (3) the five quantized values  $q_i = (H_{i+1}/H_i)$  of the five most dominant harmonic ratios (3 : 2), (5 : 3), (2 : 1), (5 : 2), (3 : 1) for the harmonic orbit resonance model. Although we narrowed down the possible harmonic ratios to five values, there is no theory that predicts in what order these five values are distributed for a given number of planets or moons. Among the many possible permutations (e.g.,  $5^{10} \approx 10^7$  for 10 planets), we make a model with the simplest choice of including a first-order term  $\Delta q$ , besides the zero-order constant  $q_i$ ,

$$\left(\frac{T_{i+1}}{T_i}\right) = q_i = q_1 + (i - 1) \Delta q, \quad i = 1, \dots, n_p, \quad (15)$$

which simply represents a linear gradient of the time period progression factor  $q_i$  for each planet. The corresponding geometric progression factor is according to Kepler's law (Eq. 3),

$$\left(\frac{R_{i+1}}{R_i}\right) = Q_i = [q_1 + (i - 1) \Delta q]^{2/3}, \quad i = 1, \dots, n_p. \quad (16)$$

For a given set of observations with time periods  $T_i, i = 1, \dots, n_p$ , we can then fit the model of Eq. (15) by minimizing the residuals  $|T_i^{\text{model}}/T_i^{\text{obs}} - 1|$ , in order to determine the gradient  $\Delta q$ . If the geometric progression factor is a constant, as assumed in the generalized Titius-Bode law, the term will vanish, i.e.,  $\Delta q = 0$ , while it will be non-zero for any other model. We anticipate that the term  $\Delta q$  will be positive, because a negative value would reverse the planet distances for high planet numbers. If the geometric progression factor is monotonically increasing with the planet number, we expect the lowest admitted harmonic value of  $q_1 = (3/2) = 1.5$  for the first planet, and the highest admitted harmonic value of  $q_n = (3/1) = 3.0$  for the outermost planet  $n$ . We will describe the results of the data fitting in Section 3. Once we determined the functional form of the progression factor  $q_i$ , we can then easily find missing planets or moons based on the theoretical progression factors predicted by the model of Eq. (16).

## 2.6. Self-Organization of Planet Distances

We interpret now the evolution of the most stable planet orbits as a self-organizing process, which produces a regular geometric pattern that we characterize with the geometric ( $Q_i$ ) or temporal progression factor  $q_i$ . A constant factor  $Q_i$  corresponds to a strictly logarithmic spacing, because the planet distance increases by a constant factor for each iterative planet number. The previously described steps of the theory

concern mostly the calculation of the specific geometric pattern of the planet distances. Let us justify now the interpretation in terms of a self-organizing system.

Self-organizing systems create a spontaneous order, where the overall order arises from local interactions between the parts of the initially disordered system. In the case of our solar system, the initially disordered state corresponds to the state of the solar system formation by self-gravity, where the local molecular cloud condenses into individual planets that form our solar system. The self-organization process is spontaneous and does not need control by any external agent. In our solar system, it is the many gravitational disturbances that interact between all possible orbits, and finally settle (over billions of years) into the most stable orbits that result from harmonic orbit resonances, as observed in our solar system (Peale 1976). A self-organizing system is triggered by random fluctuations, and then amplified by a positive feedback. The positive feedback in the evolution of planet orbits is given by the stabilizing gravitational interactions in resonant orbits, while a negative feedback would occur when a gravitational disturbance pulls a planet out of its orbit, or during a migration phase of planets, where marginally stable orbits can be disrupted. A self-organizing system is not controlled from outside, but rather from all interacting interior parts. Thus, a 10-planet system results from the evolution of  $10 \times 10 = 100$  two-body interactions, which obviously lead to a self-organized equilibrium, unless large exterior disturbances occur (e.g., a passing star or a migrating Jupiter), or if there is not sufficient critical mass to condense to a full planet in the initial phase. The asteroids represent such an example of incomplete condensation, prevented by the gravitational tidal forces of the nearby Jupiter. Finally, a self-organizing system is robust and survives many small disturbances and can self-repair substantial perturbations. Thus, a solar system, or a moon system of a planet, appears to fulfill all of these general properties of a self-organizing system.

### 3. OBSERVATIONS AND DATA ANALYSIS

#### 3.1. The Planets in our Solar System

In Fig. 4 we show the distances  $R$  of the planets to the Sun in our solar system, as predicted with the Titius-Bode law (Fig. 4a), juxtaposed to the so-called generalized Titius-Bode law (Fig. 4b), and the harmonic orbit resonance model (Fig. 4c). Although the Titius-Bode law fits the observed planet distances very well from Venus ( $n = 2$ ) to Uranus ( $n = 8$ ), it breaks down at the most extremal ranges. For Mercury ( $n = 1$ ), it would predict a distance of  $R_1 = 0.55$  rather than the observed value of  $R_1 = 0.387$ , and thus it had been set ad hoc to a value of  $R_1 = 0.4$  in the Titius-Bode law (Eq. 1). For Neptune ( $n = 9$ ) and Pluto ( $n = 10$ ) the largest deviations occur. For Pluto, a value of  $R_{10} = 77.2$  AU is predicted, while the observed value is  $R_{10} = 39.48$  AU, which is an over-prediction by almost a factor of two. In the overall, the Titius-Bode law agrees with the observations within a mean and standard deviation of  $R_{pred}/R_{obs} = 1.18 \pm 0.31$  (Fig. 4a).

The generalized Titius-Bode law (Fig. 4b) shows a better overall agreement of  $R_{pred}/R = 0.95 \pm 0.13$ , which is a factor of 2.4 smaller standard deviation than the Titius-Bode law. We fitted the data with a constant progression factor  $Q = R_{n+1}/R_n$  and found a best-fit value of  $Q = 1.72$ . Some improvement over the original Titius-Bode law is that there is no excessive mismatch for the nearest planet (Mercury,  $n = 1$ ) or the outermost planets (Neptune  $n = 9$  and Pluto  $n = 10$ ), although the Titius-Bode law fits somewhat better for the mid-range planets (from Venus to Uranus).

A significantly better agreement between the observed planet distances  $R$  and model-predicted values  $R_{pred}$  is achieved by using the harmonic ratios as determined from the resonance condition for each planet

(Eq. 14 and Fig. 3), yielding an accuracy of  $R_{pred}/R = 1.00 \pm 0.04$  (Fig. 4c), which is a factor of 8 better than the original Titius-Bode law, and a factor of 3 better than the generalized Titius-Bode law. The distance values predicted by the different discussed models are compiled for all 10 planets in Table 2. Note that a better agreement between the model and the data is achieved with the quantized harmonic ratios  $q_i$ , rather than using the logarithmic spacing assumed in the generalized Titius-Bode law.

Is there an ordering scheme of the harmonic ratios  $q_i$  in the sequence of planets  $i = 1, \dots, n$ ? From the harmonic ratios displayed in Fig. 4c and Table 2 it becomes clear that there is a tendency that the harmonic ratios  $q_i$  increase with the ordering number  $i$  of a planet, with two exceptions out of the 10 planets. The first exception is the interval between Mercury and Venus, where an additional planet can be inserted, while the second exception is the planet Neptune, which can be eliminated and then produces a pattern of monotonically increasing intervals. We apply this modification in Fig. 5 and fit then our theoretical model with a linearly increasing progression factor (Eq. 15, 16). We see that a linearly increasing progression factor yields a best fit with an accuracy of  $R_{pred}/R_{obs} = 0.96 \pm 0.04$ , or 4% (Fig. 5a). The best fit yields a linear increment of  $q = 0.205$  and a harmonic range of  $q = 1.40 - 3.24$  (Fig. 5b), close to the theoretically predicted range of  $q = 1.5 - 3.0$  for the allowed five dominant harmonic ratios. Thus we can conclude that the self-organized pattern is consistent with a linearly increasing progression factor, at least for 8 out of the 10 planets.

It is interesting to speculate on the reason of the two mismatches. The observed harmonic ratio of Neptune-Pluto (3:2) and Uranus-Neptune (2:1) yields a ratio of  $(3:2) \times (2:1) = (3:1)$ , which perfectly fits the theoretical model and is one of the allowed harmonic ratios. Therefore, Neptune occupies a stable orbit between Uranus and Pluto, which does not match the primary progressive geometric pattern, but fits a secondary harmonic pattern. Neptune might have joined the solar system later, or survived on a stable, interleaved harmonic orbit. It also might have to do with the crossing orbits of Neptune and Pluto. The second exception is a missing planet between Mercury and Venus, based on the regular pattern of a linearly increasing progressive ratio  $q$  (Eq. 15, 16). The observed harmonic ratio is (5:2) between Mercury and Venus, which can be subdivided into two harmonic ratios  $(5:3) \times (3:2) = (5:2)$  to match our theoretical pattern (Eq. 15, 16) of a monotonically increasing harmonic ratio. Consequently, a planet orbit between Mercury and Venus is expected in order to have a regular spacing, which could have been occupied by an earlier existing planet that was pulled out later, or this predicted harmonic resonance zone was never filled with a planet.

What are the predictions for a hypothetical planet outside Pluto? The Titius-Bode law is unable to make a prediction, because it over-predicts the distance of Pluto already by a factor of 2, and thus an even larger uncertainty would be expected for a trans-Plutonian planet. The harmonic orbit resonance model, using a geometric mean extrapolation method, predicts a orbital period of  $T_{n+1} \approx T_n^2/T_{n-1} = 975$  yrs and a distance of  $R_{n+1} = R_n(T_{n+1}/T_n)^{2/3} = 80$  AU for the next trans-Plutonian planet. A known object in proximity is the Kuiper belt which extends from Neptune (at 30 AU) out to approximately 50 AU from the Sun, which overlaps with Pluto, but not with the predicted distance of a trans-Plutonian planet. Another nearby object is Eris, the most massive and second-largest dwarf planet known in our solar system (Brown et al. 2005). Eris has a highly eccentric orbit with a semi-major axis of 68 AU, so it is close to our prediction of  $R_{n+1} = 80$  AU. However, since there are many more dwarf planets known at trans-Neptunian distances, they could all be part of a major ring structure, like the asteroids. In addition, the regular pattern predicted by our harmonic orbit resonance model would require a harmonic ratio larger than  $q = 3$  for a planet outside Pluto (Fig. 5b), in excess of the allowed five harmonic ratios, which is an additional argument that trans-Plutonian planets are not expected to have a stable orbit.

### 3.2. The Moons of Jupiter

A recent compilation of planetary satellites lists 67 moons for Jupiter ([http://www.windows2universe.org/our\\_solar\\_system.moons\\_table.html](http://www.windows2universe.org/our_solar_system.moons_table.html)). Only 7 out of the 67 Jupiter moons have a size of  $D > 100$  km, namely Amalthea, Thebe, Io, Europa, Ganymede, Callisto, and Himalia. The smaller objects with  $1 < D < 100$  km often occur in clusters in the distance distribution, which may be fragments that never condensed to a larger moon or may be the remnants of collisional fragmentation. The irregular spacing in the form of clusters makes these small objects with  $D < 100$  km unsuitable to study regular distance patterns. Clusters of sub-planet sized bodies in the outer solar system would require additional model components, which are not accommodated here at this time.

We show a fit of the harmonic orbit resonance model to the 7 largest Jupiter moons in Fig. 6a, which matches our theoretical model (Eqs. 15, 16) with an accuracy of  $R_{pred}/R_{obs} = 1.01 \pm 0.02$ . The regular spacing is shown in Fig. 6b, where the 7 observed moon distances fit a pattern with 10 iterative harmonic ratios. The 7 moons include the 3 Galilean satellites Io, Europa, and Ganymede that were known to exhibit highly accurate harmonic ratios already by Laplace in 1829 (Eq. 9). The empty resonance zones ( $n = 3$ ,  $n = 8$ ,  $n = 9$ ) are found at distances of  $R_3 = 270$  Mm,  $R_8 = 3370$  Mm, and  $R_9 = 6100$  Mm, where we propose to search for additional Jupiter moons. The moon closest to Jupiter is Adrastea, with a distance of 128.98 km, which is close to the Roche radius (Wylie 1931), and thus no further moons are expected to be discovered in nearer proximity to Jupiter.

Since 7 moons fit a geometric pattern with 10 elements with such a high accuracy of 2% in the moon distance (to the center of the hosting planet), we have a strong argument that the underlying self-organizing mechanism based on stable harmonic orbit resonances predicts the correct pattern of moon distances, but there are holes in this geometric scheme that are not filled by moons, which apparently do not have a simple predictable pattern. Therefore, our theoretical model has a predictability of 70% for the case of Jupiter moon distances, unless there exist some un-discovered moons with diameters of  $> 100$  km, which we consider as unlikely.

### 3.3. The Moons of Saturn

The same compilation of planetary satellites mentioned above lists 62 moons for Saturn. The largest 6 moons (Enceladus, Tethys, Dione, Rhea, Titan, Iapetus) have a diameter of  $D > 400$  km and fit the harmonic orbit resonance model with an accuracy of  $R_{pred}/R_{obs} = 0.95 \pm 0.01$ . If we set the same limit of  $D > 100$  km as for Jupiter (Section 3.2), we have 13 observed moons and find a best fit of  $R_{pred}/R_{obs} = 0.95 \pm 0.06$  (Fig. 7a). Inspecting the distance spacing (Fig. 7b) we find that a geometric pattern with 11 ratios fits the data best, where two resonance zones are occupied by two moons each, and 3 resonance zones are not occupied. Nevertheless, the spatial pattern fits the data in the predicted range of harmonic ratios,  $q = 1.46 - 2.60$  (Fig. 7b).

### 3.4. The Moons of Uranus

For Uranus, a total of 27 moons have been discovered so far, of which 8 moons have a diameter of  $D > 100$  km. Seven of the 8 largest moons have a quasi-periodic pattern, while Sycorax is located much further outside (Fig. 8). The best-fit geometric pattern shows 12 resonant zones (Fig. 8b), which fit the

observed moon distances with an accuracy of  $R_{pred}/R_{obs} = 0.97 \pm 0.07$  (Fig. 8a). The range of best-fit harmonics  $q = [1.50 - 2.71]$  (Fig. 8b) is close to the theoretical prediction  $q = [1.5 - 3.0]$ .

### 3.5. The Moons of Neptune

A total of 14 moons have been reported for Neptune, of which 6 have a diameter of  $D > 100$  km (Fig. 9), namely Galatea, Despina, Larissa, Proteus, Triton, and Nereid. We show the distances of these 6 moons to the center of Neptune in Fig. 9. The harmonic resonance model fits the 6 moons with an accuracy of  $R_{pred}/R_{obs} = 1.03 \pm 0.06$  (Fig. 9a). The range of best-fit harmonics is  $q = [1.29 - 3.55]$  (Fig. 9b), close to the theoretical prediction  $q = [1.5 - 3.0]$ .

### 3.6. Exo-Planets

Five hypothetical planetary positions were measured in the 55 Cancri system, located at distances of 0.01583, 0.115, 0.240, 0.781, and 5.77 AU from the center of the star (Cuntz 2012). Cuntz (2012) applied the Titius-Bode law and predicted 4 intermediate planet positions at 0.081, 0.41, 1.51, and 2.95 AU, adding up to a 9-planet system. A similar prediction was made by Poveda and Lara (2008), predicting two additional planets at 2.0 and 15.0 AU. Applying the harmonic resonance model to this data (Fig. 10), which yields a best fit with an accuracy of  $R_{pred}/R_{obs} = 1.01 \pm 0.07$  and predicts a total of 12 planets with 7 unknown positions at  $R_2 = 0.022$ ,  $R_3 = 0.031$ ,  $R_4 = 0.048$ ,  $R_5 = 0.077$ ,  $R_8 = 0.40$ ,  $R_{10} = 1.46$ , and  $R_{11} = 2.93$  AU. It is gratifying to see that the later four positions predicted by our model, e.g.,  $R = 0.077, 0.40, 1.46, 2.93$  AU, agree well with the predictions of Cuntz (2012), e.g.,  $R = 0.081, 0.41, 1.51, 2.95$  AU. Our harmonic orbit resonance model predicts in total a number of 12 planets within the harmonic ratio range of  $q = [1.61 - 3.11]$  (Fig. 10b), where 7 planets are un-discovered.

In the millisecond pulsar PSR 1257+12 system, two planet companions were discovered (Wolszczan and Frail 1992), at distances of  $R_1 = 0.36$  AU and  $R_2 = 0.47$ , for which the Titius-Bode law has been applied to predict additional planets (Bisnovatyi-Kogan 1993). The orbital distance ratio is  $R_2/R_1 = 1.31$  and implies (using Kepler’s law) an orbital period ratio of  $T_2/T_1 = (R_2/R_1)^{3/2} = 1.50$  that exactly corresponds to the harmonic ratio  $(H_2 : H_1) = (3/2)$ , and thus is fully consistent with the harmonic orbit resonance model.

The HRPS search for southern extra-solar planets discovered seven periods in the star HD 10180 (Lovis et al. 2011), which can be translated into distances of exo-planets from the central star by using Kepler’s law and are plotted in Fig. 11a. We find a total of 11 planets that fit the harmonic resonance model with an accuracy of  $R_{pred}/R_{obs} = 0.97 \pm 0.10$  and we predict four undiscovered planets in the resonant rings  $n = 2, 3, 5, 9$  with distances of  $R_2 = 0.029$ ,  $R_3 = 0.039$ ,  $R_8 = 0.089$ , and  $R_{10} = 1.55$  AU.

In the eclipsing polar HU Aqr, two orbiting giant planets at distances of  $R_1 = 3.6$  and  $R_2 = 5.4$  AU were discovered (Qian et al. 2011). The ratio is  $Q = 5.4/3.6 = 1.50$  implies a period ratio of  $q = Q^{3/2} = 1.84$  which is not close to a harmonic ratio.

The application of the Titius-Bode to exo-planet data furnished 141 additional exoplanets in 68 multiple-exoplanet systems (Bovaird and Lineweaver 2013). In a follow-up study, Bovaird et al. (2015) predicted the periods of 228 additional planets in 151 multi-exoplanet systems. Huang and Bakos (2014) searched in *Kepler* Long Cadence data for the 97 predicted planets of Bovaird and Lineweaver (2013) in 56 of the multi-planet systems, but found only 5 planetary candidates around their predicted periods and questioned the prediction

power of the Titius-Bode law.

### 3.7. Statistics of Results

We summarize the statistics of results in Table 3. The analyzed data set consists of our solar system, four moon systems (Jupiter, Saturn, Uranus, and Neptune), and two exo-planet systems. We found that each of these 7 systems consisted of  $N_{res} = 10 - 12$  resonant zones, of which  $N_{occ} = 5 - 10$  were occupied with detected satellites, while  $N_{miss} = 0 - 7$  resonant zones were not occupied by sizable moons (with diameters of  $D > 100$  km) or detected exo-planets. For the two exo-planet systems we predict 11 additional resonance zones that could harbor planets (Table 4).

The new result that each planet or moon system is found to have about 10 resonant ring zones indicates some unknown fundamental law for the maximum distance limit of planet or moon formation. The innermost distance is essentially given by the Roche limit, while the outermost distance may be related to an insufficient mass density that is needed for gravitational condensation. Our empirical result predicts a distance range of  $R_{10}/R_1 \approx 130$  for a typical satellite system with  $N_{res} \approx 10$  satellites. The relationship between the number of satellites and the range of planet (or moon) distances is directly connected to the variation of the progression factors, which is summarized in Fig. 12 for all 7 analyzed systems.

## 4. DISCUSSION

### 4.1. Quantized Planet Spacing

The distances of the planets from the Sun, as well as the distances of the moons from their central body (Jupiter, Saturn, Uranus, Neptune) have been fitted with the original Titius-Bode law, using a constant geometric progression factor with empirical values in the range of  $Q = R_{i+1}/R_i = 1.26 - 2.0$  (Table 1), with the Schrödinger-Bohr atomic model,  $R_n \propto n(n+1) \approx n^2$ , Wylie 1931; Louise 1982; Scardigli 2007a,b), or with more complicated polynomial functions (e.g., Blagg 1913).

The assumption of a constant geometric progression factor in the planet distances, which corresponds to a regular logarithmic spacing, is apparently incorrect, based on the poor agreement with observations, while the harmonic orbit resonance model has the following properties: (1) It fits the planet distances with 5 quantized values (that relate to the five dominant harmonic ratios) with a much higher accuracy than the Titius-Bode law and its generalized version; (2) It is based on the physical model of harmonic orbit resonances, and (3) disproves the assumption of a constant progression factor (which corresponds to a logarithmic spacing). In contrast, it predicts variations between neighbored orbital periods from  $q_{min} = 1.5$  to  $q_{max} = 3.0$ , which amounts to variations by a factor of two. The harmonic orbit resonance model fits the data best for a linearly increasing progression factor, starting from  $q_1 = q_{min} = (3 : 2) = 1.5$  for the first (innermost) planet pair, and ending with  $q_n = q_{max} = (3 : 1) = 3.0$  for the last (outermost) planet pair. From the 7 different data sets analyzed here we find the following mean values:  $\Delta q = 0.16 \pm 0.05$  for the linear gradient of the time period progression factor,  $q_{min} = 1.45 \pm 0.10$  for the minimum progression factor, and  $q_{max} = 3.00 \pm 0.33$  for the maximum progression factor (Table 3). If we use the mean value of  $\Delta q = 0.16$ , the model (Eq. 15) predicts the following ratios for a sample of 10 planets:  $q_1 = 1.50$ ,  $q_2 = 1.66$ ,  $q_3 = 1.82$ ,  $q_4 = 1.98$ ,  $q_5 = 2.14$ ,  $q_6 = 2.30$ ,  $q_7 = 2.46$ ,  $q_8 = 2.62$ ,  $q_9 = 2.78$ ,  $q_{10} = 2.94$ , Rounding these values to the next allowed harmonic number (which is a rational number), the following sequence of harmonic ratios

is predicted:  $q_1 = (3 : 2)$ ,  $q_2 = (5 : 3)$ ,  $q_3 = (5 : 3)$ ,  $q_4 = (2 : 1)$ ,  $q_5 = (2 : 1)$ ,  $q_6 = (5 : 2)$ ,  $q_7 = (5 : 2)$ ,  $q_8 = (5 : 2)$ ,  $q_9 = (3 : 1)$ ,  $q_{10} = (3 : 1)$ , which closely matches the sequence of observed harmonic resonances (Table 2, column 4) in our solar system. These harmonic ratios match the observations closely, and thus provide an adequate description of the geometric pattern created by the self-organizing system.

#### 4.2. The Geometric Progression Factor

Several attempts have been made to find a theoretical physical model for the empirical Titius-Bode law. There exists no physical model that can explain the mathematical function that was empirically found by Titius and Bode, with a scaling relationship  $2^{(n-2)}$ , multiplied by an arbitrary factor and an additive constant (Eq. 1). One interpretation attempted to relate it to the Schrödinger-Bohr atomic model,  $R_n \propto n(n+1) \approx n^2$ , Wylie 1931; Louise 1982; Scardigli 2007a,b), but the reason why it was found to fit the Titius-Bode law is simply because both series scale similarly for small integer numbers, i.e.,  $2^n \propto 1, 2, 4, 8, 16, 32, \dots$  versus  $n^2 \propto 0, 1, 4, 9, 16, 25, \dots$ , but this numerological coincidence does not imply that atomic physics and celestial mechanics can be understood by the same physical mechanism, although both exhibit discrete quantization rules.

Most recent studies assume that the physics behind the Titius-Bode law is related to the accretion of mass through collisions within a protoplanetary disk, clearing out material in orbits with harmonic resonances, which leads to a non-random distribution of planet orbits with roughly logarithmic spacing (e.g., Peale 1976; Hayes and Tremaine 1998; Bovaird and Linewaver 2013). Quantitative modeling of such a scenario is not easy, because it implies Monte Carlo-type N-body simulations of a vast number of planetesimals that interact with  $N^2$  mutual gravitational terms. Analytical solutions of N-body problems, as we know since Lagrange, are virtually non-existent for  $N \geq 3$ . However, the configuration of planets that we observe after a solar system life time of several billion years suggests that the observed harmonic orbit resonances represent the most stable long-term solutions of a resonant system, otherwise the solar system would have disintegrated long ago.

In contrast to the generalized Titius-Bode law with logarithmic spacing, we argue for a model with quantized geometric progression factors, based on the most relevant harmonic ratios that stabilize resonant orbits. From a statistical point of view we can understand that there is a “sweet spot” of harmonic ratios in the planet orbits that is not too small (because it would lengthen the conjunction times and reduce the frequency of gravitational interactions necessary for the stabilization of orbits), and is not too large (because the inter-planet distances at conjunction would be larger and the gravitational force weaker). These reasons constrain the optimum range of dominant harmonic ratios, for which we found the 5 values between  $(3/2)$  and  $(3/1)$ . However, there are still open questions why there is a linear gradient  $\Delta q$  in the orbit time (and geometric) progression factor, and what determines the value of this gradient  $\Delta q \approx 0.16$ . The specific value of the gradient determines how many planets  $n_p$  can exist in a resonant system within the optimum range of harmonic numbers (from  $q_{min} = 1.5$  to  $q_{max} = 3$ ). (Fig. 12). Therefore, since we have no theory to predict the gradient  $\Delta q$ , we have to resort to fitting of existing data and treat the gradient  $\Delta q$  as an empirical variable.

### 4.3. Self-Organizing Systems

One necessary property of self-organizing systems is the positive feedback mechanism. Solar granulation (Fig. 1a), for instance, is driven by subphotospheric convection, a mechanism that has a vertical temperature gradient in a gravitationally stratified layer. It is subject to the Rayleigh-Bénard instability, which can be described with three coupled differential equations, the so-called Lorenz model (e.g., Schuster 1988). The positive feedback mechanism results from the upward motion of a fluid along a negative vertical temperature gradient, which cools off the fluid and makes it sink again, leading to chaotic motion. In the limit cycle, which is a strange attractor of this chaotic system, the system dynamics develops a characteristic size of the convection cells (approximately 1000 km for solar granulation), which is maintained over the entire solar surface by this self-organizing mechanism of the Lorenz model.

For planet orbits, gravitational disturbances act most strongly between planet pairs that have a harmonic ratio of their orbit times, because the gravitational pull occurs every time at the same location for harmonic orbits. Such repetitive disturbances that occur at the same location into the same direction will pull the planet with the lower mass away from its original orbit and make its orbit unstable. However, if there is a third body with another harmonic ratio at an opposite conjunction location, it can pull the unstable planet back into a more stable orbit. This is a positive feedback mechanism that self-organizes the orbits of the planets into stable long-term configurations. A more detailed physical description of the resonance phenomenon can be found in the review of Peale (1976).

### 4.4. Random Pattern Test

A prediction of the harmonic orbit resonance model is that the the spacing of stable planet orbits is not random, but rather follows some quasi-regular pattern, which we quantified with the quantized spacing given with Eqs. (15, 16). However, the matching of the observed planet distances with the resonance-predicted pattern is not perfect, but agrees within an accuracy of  $R_{pred}/R_{obs} = 1.00 \pm 0.06$  in the statistical average only (Table 3), the question may be asked whether a random process could explain the observed spacing. In order to test this hypothesis we performed a Monte-Carlo simulation with 1000 random sets of planet distances and analyzed it with the same numerical code as we analyzed the observations shown in Figs. (4-11). In Fig. 13 we show a 2D distribution of two values obtained for each of the 1000 simulations: The y-axis shows the standard deviation  $|R_{model}/R_{sim} - 1|$  of the ratio of modeled and simulated values of planet distances, which is a measure of how well the model fits the data; The x-axis shows the deviations  $[(q_{min} - 1.5)^2 + (q_{max} - 3.0)^2]^{1/2}$  of the best-fit progression factors  $q_{min}$  and  $q_{max}$  (added in quadrature), which is a measure how close the simulated and theoretically predicted progression factors agree. From the 2D distribution shown in Fig. 13 we see that the data set of Jupiter matches the model best and exhibits the largest deviation from the random values, while the other six 6 data sets are all distributed at the periphery of the random values. Nevertheless, all analyzed data sets are found to be significantly different from random spacing of planet or moon distances.

### 4.5. Exo-Planet Searches

The Titius-Bode law was also applied to exo-planets of stellar systems, such as the solar-like G8 V star 55 Cnc (Cuntz 2012; Poveda and Lara 1980), the millisecond pulsar PSR 1257+12 system (Bisnovatyi-Kogan 1993), the star HD 10180 (Lovis et al. 2011), the eclipsing polar HU Aqr (Qian et al. 2011), and to over 150

multi-planet systems observed with Kepler (Bovaird and Lineweaver 2013; Bovaird et al. 2015; Huang and Bakos 2014). The search in Kepler data, however, did not reveal much new detections based on predictions with the generalized Titius-Bode law, i.e.,  $R_n = R_1 Q^n$  (Huang and Bakos 2014). Although a similar iterative formulation is used in both the generalized Titius-Bode law and the harmonic resonance model (Eq. 6, 7), the geometric progression factor  $Q$  is used as a free variable individually fitted to each system in other studies (e.g., Bovaird and Lineweaver 2013).

The question arises how the harmonic orbit resonance model can improve the prediction of exo-planet candidates. The two examples shown in Figs. (10-11) suggest that the predicted spatio-temporal pattern can be fitted to incomplete sets of exo-planets with almost equal accuracy as the data sets from the (supposedly complete) data sets in our solar system. This may be true if there are  $\gtrsim 5$  planets detected per star, but it may get considerably ambiguous for smaller sets of  $\approx 2-4$  exo-planets per star. However, since the harmonic orbit resonance model predicts a variable ratio of the time period progression factor that fits existing data, it should do better than the generalized Titius-Bode law with a constant progression factor, as it was used in recent work (Bovaird and Lineweaver 2013; Bovaird et al. 2015).

## 5. CONCLUSIONS

The physical understanding of the Titius-Bode law is a long-standing problem in planetary physics since 250 years. In this study we interpret the quasi-regular geometric pattern of planet distances from the Sun as a result of a self-organizing process that acts throughout the life time of our solar system. The underlying physical mechanism is linked to the celestial mechanics of harmonic orbit resonances. The results may be useful for searches of exo-planets orbiting around stars. Our conclusions are:

1. The original form of the Titius-Bode law on distances of the planets to the Sun is a purely empirical law and cannot be derived from any existing physical model, although it fits the observations to some extent, but fails for the extremal planets Mercury, Neptune and Pluto. The “generalized form of the Titius-Bode law” assumes a constant geometric progression factor  $Q = R_{i+1}/R_i$ , which we find also to be inconsistent with the data, since the observed distance ratios vary in the range of  $Q \approx 1.3 - 2.1$ , corresponding to a variation of  $q = T_{i+1}/T_i \approx 1.5 - 3.0$  of the orbital periods, according to Kepler’s third law,  $q \propto Q^{3/2}$ .
2. The observed orbital period ratios  $q_i$  of the planets in our solar system correspond to five harmonic ratios,  $(H_{i+1}/H_i) = (3:2), (5:3), (2:1), (5:4), (3:1)$ , which represent the dominant harmonic orbit resonances that self-organize the orbits in the solar system. We find that the progression factor  $q_i$  for time periods follows approximately a linear function  $q_i = q_1 + (i-1)\Delta q$ ,  $i = 1, \dots, n$ , which varies in the range from the smallest harmonic ratio  $q_1 = (3 : 2) = 1.5$  of the innermost planet to  $q_n = (3 : 1) = 3.0$  for the outermost planet, with a gradient of  $\Delta q = 0.16 \pm 0.05$ . The progression of orbital periods  $T_i$  is quantized by the nearest dominant five harmonics,  $q_i = [1.5, 1.667, 2.0, 2.5, 3.0]$ . Based on these harmonic ratios of the orbital periods we predict the variation of the geometric progression factors as  $Q_i = [q_1 + (i-1)\Delta q]^{2/3}$ , which is also quantized,  $Q_i = q_i^{2/3} = [1.31, 1.40, 1.59, 1.84, 2.08]$ .
3. Fitting the geometric progression factors predicted by our harmonic orbit resonance model to observed data from our solar system, moon systems, and exo-planet systems, we find best agreement for Jupiter moons (with an accuracy of 2%), followed by the solar system (with an accuracy of 4% for 8 out of the 10 planets). The other moon systems (of Saturn, Uranus, Neptune) and exo-planet systems (of 55 Cnc

and HD 10180) agree with a typical accuracy of 6%-7%. We demonstrated that these accuracies of predicted planet (or moon) distances are significantly different from randomly distributed (logarithmic) distances (Fig. 13). The number of resonant zones for each star or planet amounts to  $n_{res} \approx 10 - 12$ , which is comparable with the number of sizable detected moons (with a diameter of  $D \geq 100$  km) in each moon system. For the exo-planet systems we find best fits for  $n_{res} \approx 10 - 11$  resonance zones, which allows us to predict 7 missing exo-planets for the star 55 Cnc, and 4 missing exo-planets for the star HD 10180.

4. We interpret the observed quasi-regular geometric patterns of planet or moon distances in terms of a self-organizing system. Self-organizing systems (the primordial molecular cloud around our Sun) create a spontaneous order (the Titius-Bode law) from local interactions (via harmonic orbital resonances) between the internal parts (the planets or moons) of the initially disordered (solar) system. A self-organizing process is spontaneous and does not need an external control agent. Initial fluctuations are amplified by a positive feedback (by the gravitational interactions that lead to long-term stable orbits via harmonic orbit resonances). A self-organizing system is robust (during several billion years in our solar system) and capable of self-repair after large disturbances (for instance by a passing star or a migrating giant planet, thanks to the stabilizing gravitational interactions of harmonic orbit resonances). We find that the ordered patterns of planet orbits is not always complete (a planet between Mercury and Venus seems to be missing) and can display defects (the “superfluous” Neptune, similarly to defects in crystal growth). The predicted geometric pattern thus has a high statistical probability, but is not always perfectly created in self-organizing systems.

The present study can be applied in two ways: (1) predictions of un-discovered exo-planets in other stellar systems; and (2) prediction of resonant orbits and solutions with long-term stability in numerical N-body simulations. The validity of the presented model could be corroborated by new discoveries of predicted exo-planets (e.g., Boivard and Lineweaver 2013), and by measuring the geometric scaling of gaps and rings in simulated N-body accretion systems. The harmonic orbit resonance model makes a very specific prediction about five harmonic orbit and distance ratios (rather than the logarithmic spacing assumed in the generalized Titius-Bode law), which can be tested with numerical simulations. Such a quantized geometric pattern is also distinctly different from random systems (Dole 1970; Lecar 1973; Dworak and Kopacz 1997; Dworak and Kopacz 1997; Hayes and Tremaine 1998; Lynch 2003; Neslusan 2004; Cresson 2011).

Just at the time of submission of this paper, the discovery of the Trappist-1 planetary system was announced (Gillon et al. 2017, Pletser and Basano 2017; Scholkmann 2017; Aschwanden and Scholkmann 2017). This unique exoplanet system harbors 7 planets with a regular spacing that corresponds to the harmonic ratios of  $(T_{i+1}/T_i) = [1.60, 1.67, 1.51, 1.51, 1.34, 1.62]$ . It fulfills two of our three predictions: The period ratios are close to the predicted harmonic ratios (3:2)=1.5 and (5:3)=1.67, and the sequence starts with the lowest of the predicted dominant resonances, but it does not continue to the higher harmonic ratios (2:1, 5:2, 3:1). Either we are missing additional planets further out, or the particular spectral type of the central star (dwarf star M8V) favors the lowest harmonic ratios, which have the shortest conjunction times and therefore are the most stable configurations.

The author acknowledges the hospitality and partial support for two workshops on “Self-Organized Criticality and Turbulence” at the *International Space Science Institute (ISSI)* at Bern, Switzerland, during October 15-19, 2012, and September 16-20, 2013, as well as constructive and stimulating discussions (in

alphabetical order) with Sandra Chapman, Paul Charbonneau, Henrik Jeldtoft Jensen, Lucy McFadden, Maya Paczuski, Jens Juul Rasmussen, John Rundle, Loukas Vlahos, and Nick Watkins. This work was partially supported by NASA contract NNX11A099G “Self-organized criticality in solar physics”.

## REFERENCES

- Armellini, G. 1921, *Astr. Nachr.* 215, 263.
- Aschwanden, M.J., Crosby, N., Dimitropoulou, M., Georgoulis, M.K., Hergarten, S., McAteer, J., Milovanov, A., Mineshige, S., Morales, L., Nishizuka, N., Pruessner, G., Sanchez, R., Sharma, S., Strugarek, A., and Uritsky, V. 2016, *Space Science Reviews* 198, 47.
- Aschwanden, M.J. and Scholkmann, F. 2017, *Galaxies* (subm.)
- Badolati, E. 1982, *The Moon and the Planets* 26, 339.
- Bak, P., Tang, C., and Wiesenfeld, K. 1987, *PhRvL* 59/4, 381.
- Basano, L., and Hughes, D.W. 1979, *Nuovo Cimento C*, 2C, 505.
- Bass, R.W. and Del Popolo, A. 2005, *Internat. J. Modern Physics D*, 14, 153.
- Bisnovatyi-Kogan G.S. 1993, *A&A* 275, 161.
- Blagg, M.A. 1913, *MNRAS* 73, 414.
- Bodifee, G. 1986, *Astrophys. Space Sci.* 122, 41.
- Bovaird, T. and Lineweaver, C.H., 2013, *MNRAS* 435, 1126.
- Bovaird, T., Lineweaver, C.H., and Jacobsen, S.K. 2015, *MNRAS* 448, 3608.
- Brodetsky, S. 1914, *The Observatory* 37, 338.
- Brown, M.E., Trujillo, C.A., and Rabinowitz, D.L. 2005, *ApJ* 635, L97.
- Cen, R. 2014, *ApJL* 785/2, L21.
- Camazine, S., Deneubourg, J.L., Frank, N.R., Sneyd, J., Theraulaz, G., and Bonabeau, E. 2001, *Self-Organization in Biological Systems*, Princeton University Press.
- Cameron, A.G.W. 1973, *Icarus* 18/3, 407.
- Chapman, D.M.F. 2001a, *J. Royal Astron. Soc. Canada* 95, 135.
- Chapman, D.M.F. 2001b, *J. Royal Astron. Soc. Canada* 95, 189.
- Cresson, J. 2011, *J. Math. Phys.* 52/11, 113502.
- Cuntz, M. 2012, *PASJ* 64, 73.
- Cutteridge, O.P.D. 1962, *Nature* 196, 461.
- Dai, W.S. 1975, *Acta Astronomica Sinica* 16, 123.
- Dai, W.S. 1978, *Chinese Astronomy*, 2/2, 183.
- Dermott, S.F. 1968, *MNRAS* 141, 363.
- Dermott, S.F. 1973, *Nature* 244/132, 18.
- Dobo, A. 1981, *Astron. Nachr.* 302, 93.
- Dole, S.H. 1970, *Icarus* 13/3, 494.
- Dubrulle, B. and Graner, F. 1994, *A&A* 282, 269.
- Dworak, T.Z. and Kopacz, M. 1997, *Postepy Astron.* 45, 37.
- Estberg, G.N. and Sheehan, D.P. 1994, *Geophys Astrophys. Fluid Dynamics* 78, 211.
- Fairall, A.P. 1963, *MNRAS* 22, 108.

- Filippov, A.E. 1991, JETP Lett. 54/7, 351.
- Flores-Gutierrez, J.D. and Garcia-Guerra, C. 2001, Revista Mexicana de Astronomia y Astrofisica 47, 173.
- Geach, J.E. 2012, MNRAS 419/3, 2633.
- Georgiev, T.B. 2016, Bulgarian Astron. J. 25, 3.
- Georgoulis, M.K. 2005, Solar Phys. 228, 5.
- Gillon, M., Triaud, A.H.M.J., Demory, B.O., et al. 2017, Nature 542, 456 (23 Feb 2017).
- Goldreich, P. 1965, MNRAS, I.
- Goldreich, P. and Tremaine, S.D. 1978, Icarus 34, 240.
- Gomes, R., Deienno, R., and Morbidelli, A. 2016, arXiv preprint 1607.05111v1.
- Graner, F. and Dubrulle, B. 1994, A&A 282, 262.
- Hasegawa, A. 1985, Advances Phys. 34, 1.
- Hayes, W., and Tremaine, S. 1998, Icarus 135, 549.
- Horiuchi, R. and Sato, T. 1985, Phys. Rev. Lett. 55/8, 211.
- Hu, Z.W. and Chen, Z.X. 1987, Astron. Nachr. 308/6, 359.
- Huang, C.X. and Bakos, G.A. 2014, MNRAS 442, 674.
- Isaacman, R. and Sagan, C. 1977, Icarus 31, 510.
- Jaki, S.L. 1972a, J. History Astron. 3, 136.
- Jaki, S.L. 1972b, American J. Physics 40, =/7, 1014.
- Jenkins, B.G. 1878, Nature 19, 74.
- Kitiashvili, I.N., Kosovichev, A.G., Wray, A.A., and Mansour, N.N. 2010, ApJ 719, 307.
- Kohonen, T. 1984, *Self-organization and associative memory*, Springer: New York.
- Krishan, V. 1991, MNRAS 250, 50.
- Kunz, M.W. and Lesur, G. 2013, MNRAS 434, 2295.
- Laplace, P.S. 1829, *Mechanique Céleste*, Vols. I, IV. Boston: Hillard, Gray, Little and Wilkins.
- Lecar, M. 1973, Nature 242, 318.
- Lehn, J.M. 2002, Science 295, 2400.
- Leyser, T.B. 2001, AARv 98/3, 223.
- Leydesdorff, L. 1993, J. Social Evolutionary Systems 16, 331.
- Lissauer, J.J. and Cuzzi, J.N. 1982, AJ 87, 1051.
- Louise, R. 1982, Moon and the Planets 26, 389.
- Lovis, C., Segransan, D., Mayor, M., Udry, S., Benz, W., Bertaux, J.L., Bouchy, F., Correia, A.C.M., et al. 2011, A&A 528, A112.
- Lynch, P. 2003, MNRAS 341, 1174.
- Malkov, M.A., Diamond, P.H., and Völk, H.J. 2000, ApJ 533.
- Marcus, P.S. 1993, ARAA 31, 523.

- McFadden, L.A., Weissman, P.R., and Johnson, T.V. 1999, (second edition 2007), *Encyclopedia of the Solar System*, Academic Press, New York.
- Miller, J. 1938a, *Nature* 141, /3562, 245.
- Miller, J. 1938b, *Nature* 142, /3592, 670.
- Müller S.C. and Parisi, J. 2015, *Bottom-up self-organization in supramolecular soft matter: Principles and prototypical examples of recent advances*, Springer Series in Materials Science, Springer: New York.
- Munini, E. and Armellini, A. 1978, *Recerca di leggi empiriche etc*, *Coelum* 46, 223.
- Napier, W.McD. and Dodd, R.J. 1973, *Nature* 242, 250.
- Neslusan, L. 2004, *MNRAS* 351, 133.
- Nieto, M.M. 1970, *A&A* 8, 105.
- Nieto, M.M. 1972, *The Titius-Bode Law of Planetary Distances: Its History and Theory*, Pergamon Press, Oxford.
- Nowotny, E. 1979, *The Moon and Planets* 21, 257.
- Nyambuja, G.G. 2015, *J. Modern Phys.* 6, 1195.
- Opik, E.J. 1978, *The Moon and Planets* 18, 327.
- Ortiz, J.L., Moreno, F., Molina, A., Santos, S.P., Gutierrez, P.J. 2007, *MNRAS* 379, 1222.
- Ovenden, M.W. 1972, *Nature* 239, 5374, 508.
- Ovenden, M.W. 1975, *Vistas in Astronomy* 0018, 473.
- Patton, J.M. 1988, *Celestial Mechanics* 44, 365.
- Patterson, C.W. 1987, *Icarus* 70, 319.
- Peale, S.J. 1976, *ARAA* 14, 215.
- Pletser, V. 1986, *Earth, Moon, and Planets* 36, 193.
- Pletser, V. 1988, *Earth, Moon, and Planets* 42, 1.
- Pletser, V. 2017, *Advances in Space Research* (subm.)
- Pletser, V. and Basano, L. 2017, arXiv preprint.
- Poveda, A. and Lara, P. 2008, *Revista Mexicana de Astronomia y Astrofisica* 44, 243.
- Prentice, A.J.R. 1997, *Astron. Soc. Australia, Proc.* 3, 173.
- Prisniakov V.F. 2001, *Kosmichna Nauka i Tekhnologiya* 7, 104.
- Qian, S.B., Liu, L., Liao, W.P., Li, J., Zhu, L.Y., Dai, Z.B., He J.J., Zhao, E.G., Zhang, J., and Li, K.
- Ragnarsson, S.I. 1995, *A&A* 301, 609.
- Rawal, J.J. 1978, *Bull. Astron. Soc. India* 6, 92.
- Rawal, J.J. 1986, *Astrophys. Spac. Scie* 119, 159.
- Rawal, J.J. 1989, *J. Astrophys. Astr.* 10, 257.
- Rica, S. 1995, *Comptes Rendus de l'Academie des Sciences*, 320, /9, 489.
- Ruediger, G. and Tschaepé, R. 1988, *Gerlands Beitrage zur Geophysic*, 97/2, 97.
- Scardigli, F. 2007, *J. Phys. Conf Ser.* 67, id. 012038.

- Scardigli, F. 2007, *Foundations of Phys.* 37/8, 1278.
- Scholkmann, F. 2017, *Progress in Physics* Vol. 13, 125.
- Schuster, H.G. 1988, *Deterministic Chaos*, VCH: New York.
- Smirnow V.A. 2015, *Odessa Astron Publ.* 28, 62.
- Todd, G.W. 1938, *Nature* 141/3566, 412.
- Torbett, M., Smoluchowski, R., and Greenberg, R. 1982, *Icarus* 49, 313.
- Uzdensky, D.A. 2007, *ApJ* 671, 2139.
- Valdivia, J.A., Klimas, A., Vassiliadis, D., Uritsky, V., and Takalo, J., 2003, *SSRv* 107, 515.
- Wolszcan, A. and Frail, D.A. 1992, *Nature* 355, 145.
- Wylie, C.C. 1931, *Popular Astronomy* 39, 75.
- Yamada, M. 2007, *Phys. Plasmas* 14/5, 058102.
- Yamada, M., Kulsrud, R., and Ji, H.T. 2010, *Rev. Mod. Phys.* 82, 603.

Table 1. The values of geometric progression factors ( $Q = R_{i+1}/R_i$ ) and orbital period progression factors ( $q = Q^{3/2}$ ) of solar system data are compiled from previous publications.

Geometric progression factor $Q_i$	Orbital period progression factor $q_i$	Reference
2	2.82	Titius (1766), Bode (1772), Miller 1938a,b, Fairall (1963)
1.7275	2.27	Blagg (1913), Brodetsky (1914), Nieto 1970)
1.89	2.59	Dermott (1968, 1973)
1.52	1.87	Armellini (1921); Badolati (1982)
1.52	1.87	Munini and Armellini (1978); Badolati (1982)
1.442	1.73	Rawal (1986, 1989)
1.26	1.41	Rawal (1986, 1989)
(1.31, 1.40, 1.59, 1.84, 2.08)	(1.5, 1.667, 2.0, 2.5, 3.0)	Harmonic orbit resonance model (this work)

Table 2. Observed orbital periods  $T$  and distances  $R$  of the planets from the Sun, predicted harmonic orbit resonances ( $H_1 : H_2$ ), the Titius-Bode law  $R_{TB}$ , the generalized Titius-Bode law  $R_{GTB}$ , and predictions of the harmonic orbit resonance model  $R_{HOR}$  and ratios  $R_{HOR}/R$ .

Number	Planet	Orbital period $T$ (yrs)	Harmonic Resonance ( $H_{i+1} : H_i$ )	Distance observed $R$ (AU)	Distance TB law $R_{TB}$ (AU)	Distance GTB law $R_{GTB}$ (AU)	Distance HOR $R_{HOR}$ (AU)	Ratio HOR $R_{HOR}/R$
1	Mercury	0.241	(5:2)	0.39	0.55	0.34	0.38	0.9839
2	Venus	0.615	(5:3)	0.72	0.70	0.58	0.70	0.9701
3	Earth	1.000	(2:1)	1.00	1.00	1.00	1.00	1.0000
4	Mars	1.881	(5:2)	1.52	1.60	1.72	1.56	1.0249
5	Ceres	4.601	(5:2)	2.77	2.80	2.95	2.76	0.9982
6	Jupiter	11.862	(5:2)	5.20	5.20	5.06	5.01	0.9639
7	Saturn	29.457	(3:1)	9.54	10.00	8.69	9.43	0.9888
8	Uranus	84.018	(2:1)	19.19	19.60	14.93	19.52	1.0171
9	Neptune	164.780	(3:2)	30.07	38.80	25.63	29.97	0.9968
10	Pluto	248.400	...	39.48	77.20	44.01	38.77	0.9820

Table 3. Summary of analyzed planet and moon systems using the harmonic orbit resonance model. We include only moons with a diameter  $D > 100$  km

Central Object	Number of satellites	Number of resonant zones	Occupied zones	Missing satellites	Model accuracy	Progression factor gradient	Orbital period progression factor
	$N_{sat}$	$N_{res}$	$N_{occ}$	$N_{miss}$	$R_{pred}/R_{obs}$	$dq$	$q$
Sun	10	10	10	0	$0.96 \pm 0.04$	0.205	1.40-3.24
Jupiter	7	10	7	3	$1.01 \pm 0.02$	0.161	1.41-2.85
Saturn	13	11	8	3	$0.95 \pm 0.06$	0.114	1.46-2.60
Uranus	8	12	8	4	$0.97 \pm 0.07$	0.110	1.50-2.71
Neptune	6	10	6	4	$1.03 \pm 0.06$	0.251	1.29-3.55
55 Cnc	5	12	5	7	$1.01 \pm 0.07$	0.137	1.61-3.11
HD 10180	7	11	7	4	$0.97 \pm 0.10$	0.152	1.46-2.98
mean					$1.00 \pm 0.06$	$0.16 \pm 0.05$	$1.45 \pm 0.10$ $3.00 \pm 0.33$

Table 4. Predicted exo-planets of the star 55 Cnc and HD 10180.

Central Object	Number of harmonic orbit	Predicted distance	Predicted by Cuntz (2002)
55 Cnc	2	0.022 AU	...
55 Cnc	3	0.031 AU	...
55 Cnc	4	0.048 AU	...
55 Cnc	5	0.077 AU	0.081 AU
55 Cnc	8	0.40 AU	0.41 AU
55 Cnc	10	1.46 AU	1.51 AU
55 Cnc	11	2.93 AU	2.95 AU
HD 10180	2	0.029 AU	...
HD 10180	3	0.039 AU	...
HD 10180	8	0.089 AU	...
HD 10180	10	1.55 AU	...

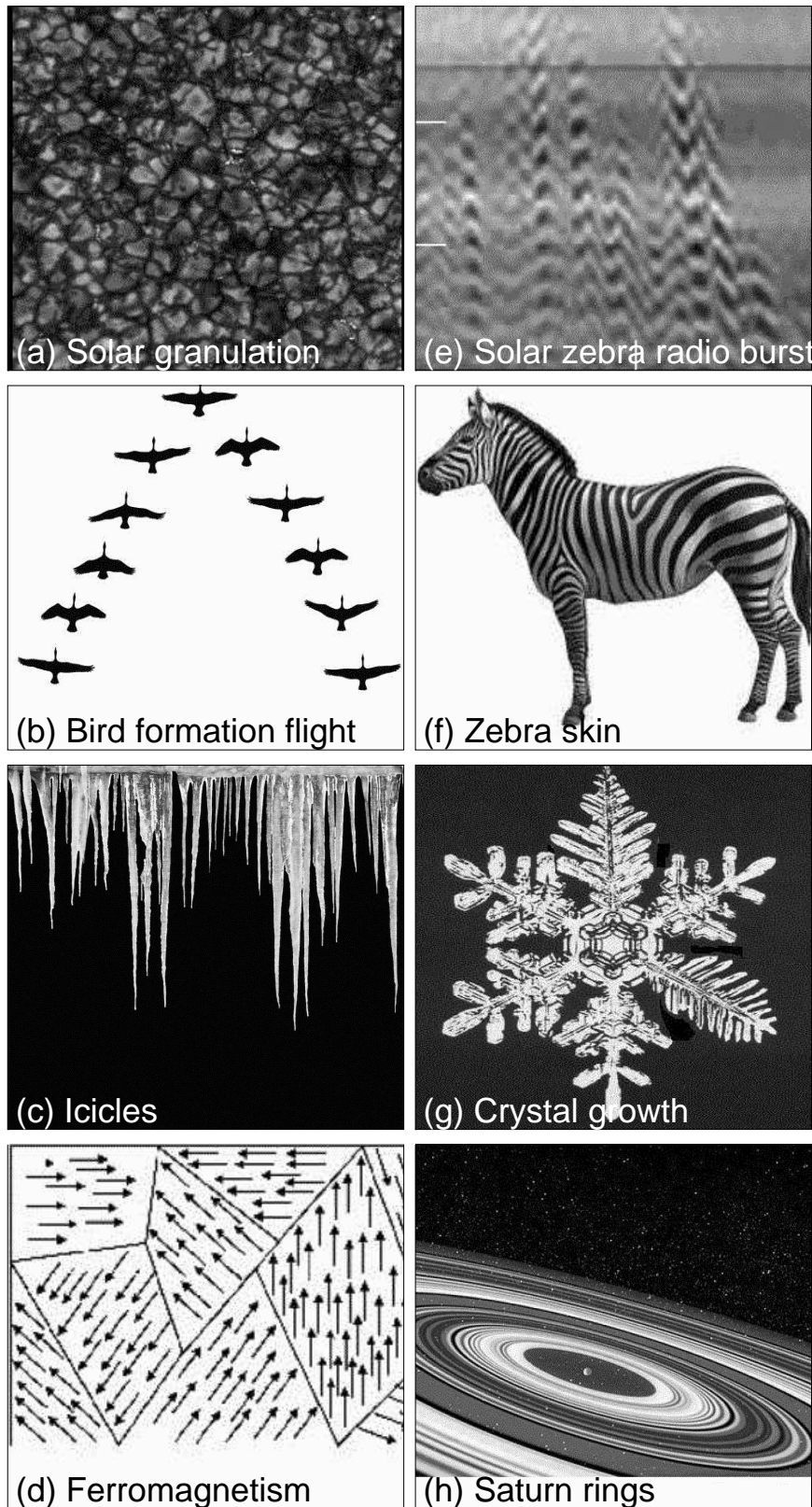


Fig. 1.— Examples of self-organizing systems: (a) Solar granulation, (b) Bird formation flight, (c) Icicles, (d) Ferromagnetism, (e) Solar zebra radio bursts, (f) Zebra skin, (g) Crystal growth, and (h) Saturn rings.

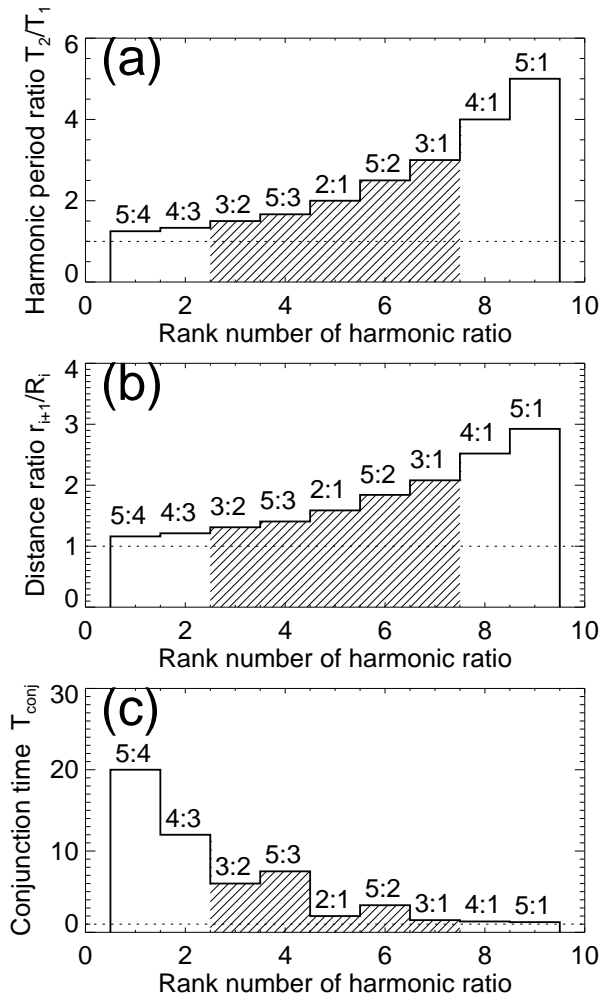


Fig. 2.— (a) Harmonic period ratios; (b) Distance ratios of planets from Sun; (c) Conjunction time. The most dominant harmonic ratios are marked with hatched line style.

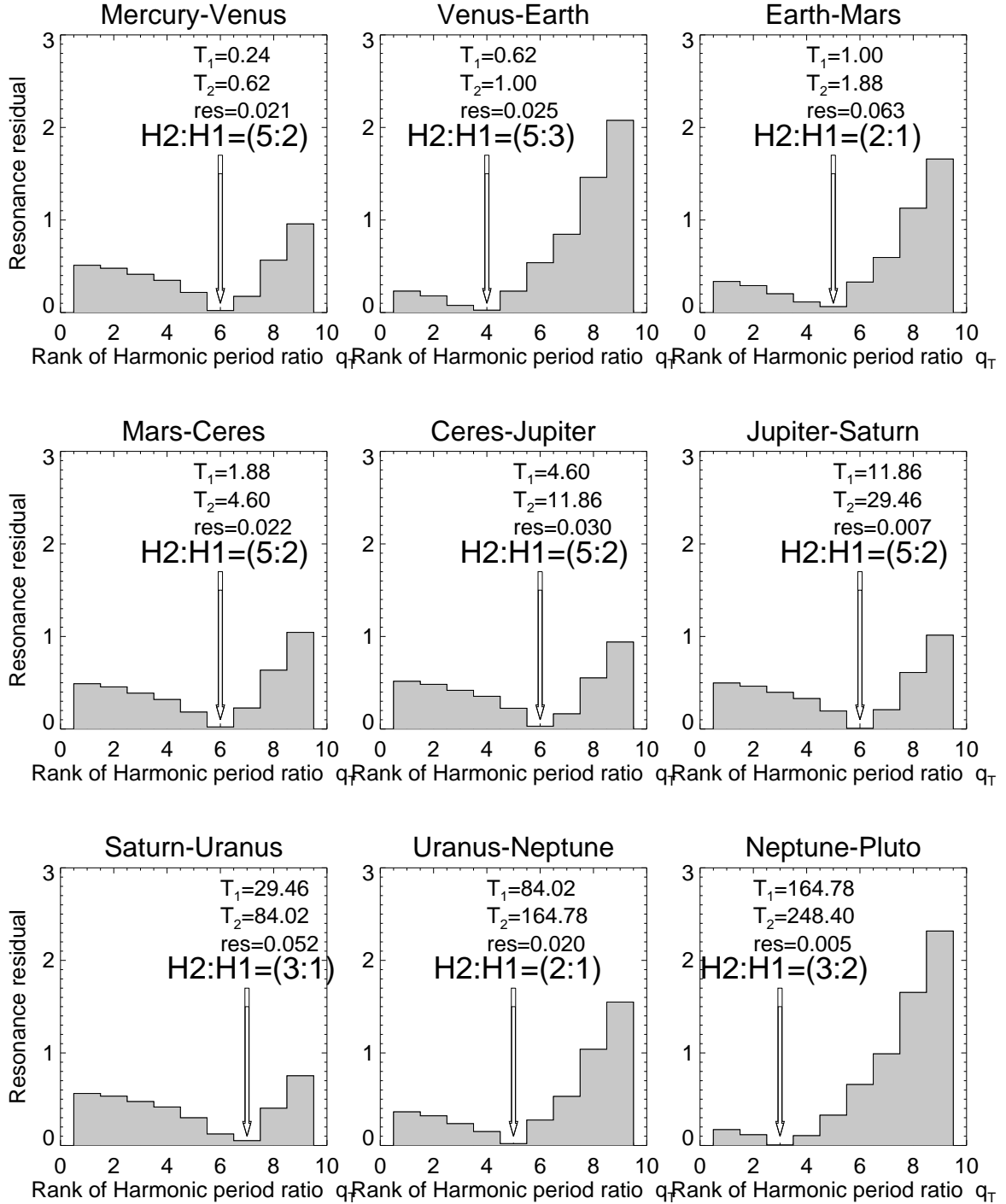


Fig. 3.— The harmonic period ratio  $H_2:H_1$  is predicted based on the minimum of the resonance condition residuals  $\omega_{min}$  (y-axis) as a function of the (rank number of the) harmonic period ratios  $q_T = T_2/T_1$  (x-axis), for the 9 planet pairs (with orbital time periods  $T_1$  and  $T_2$ ) in our solar system. The relationship between the rank number (x-axis) and the period ratio  $q_T$  is given in Fig. 2a. Note that a minimum with a singular value of  $\omega_{min} < 0.05$  exists in all 9 cases.

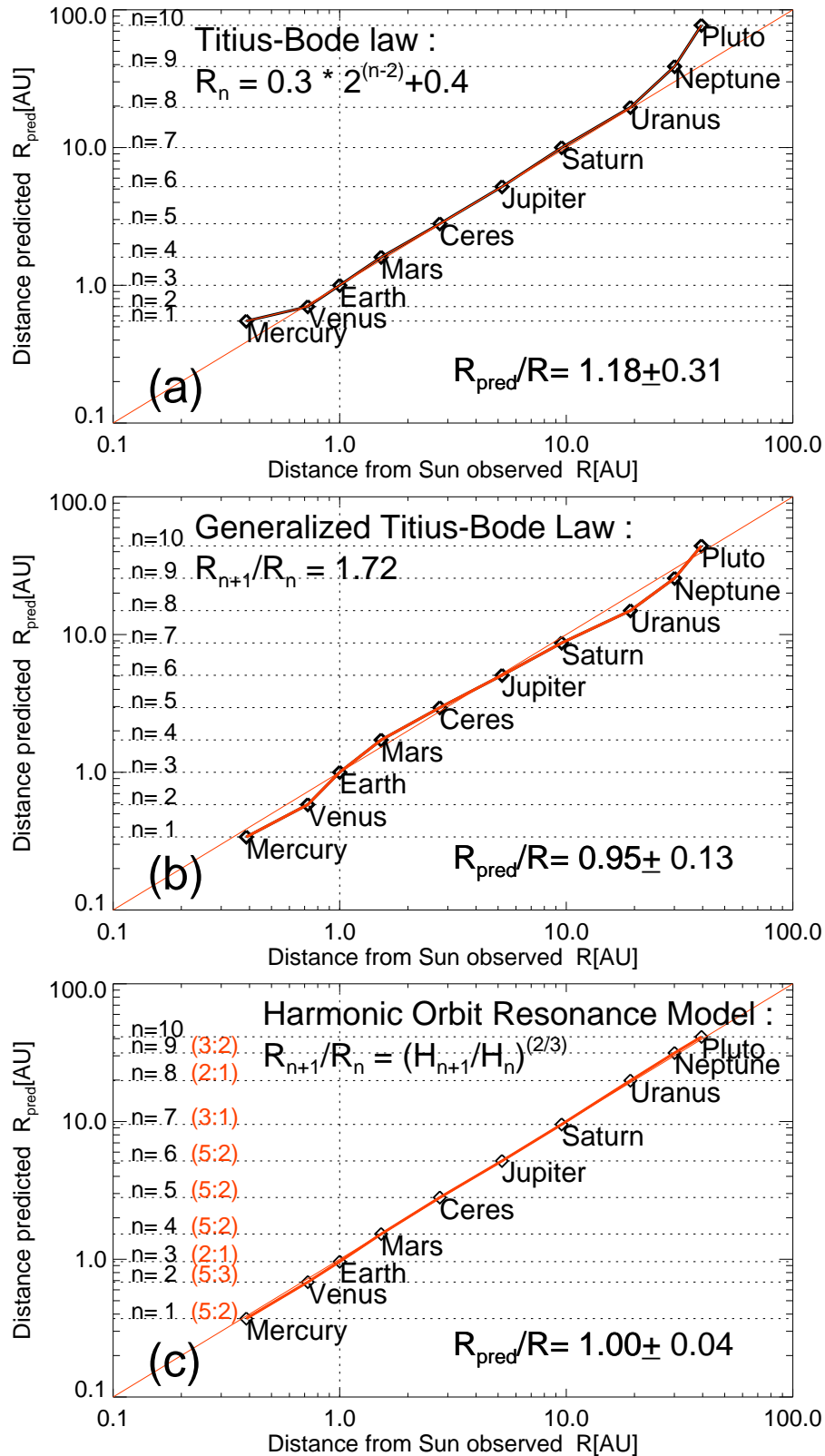


Fig. 4.— (a) The empirical Titius-Bode law of planet distances from the Sun; (b) The generalized Titius-Bode law with a constant progression factor  $Q = 1.72$ ; (c) The harmonic orbit resonance model.

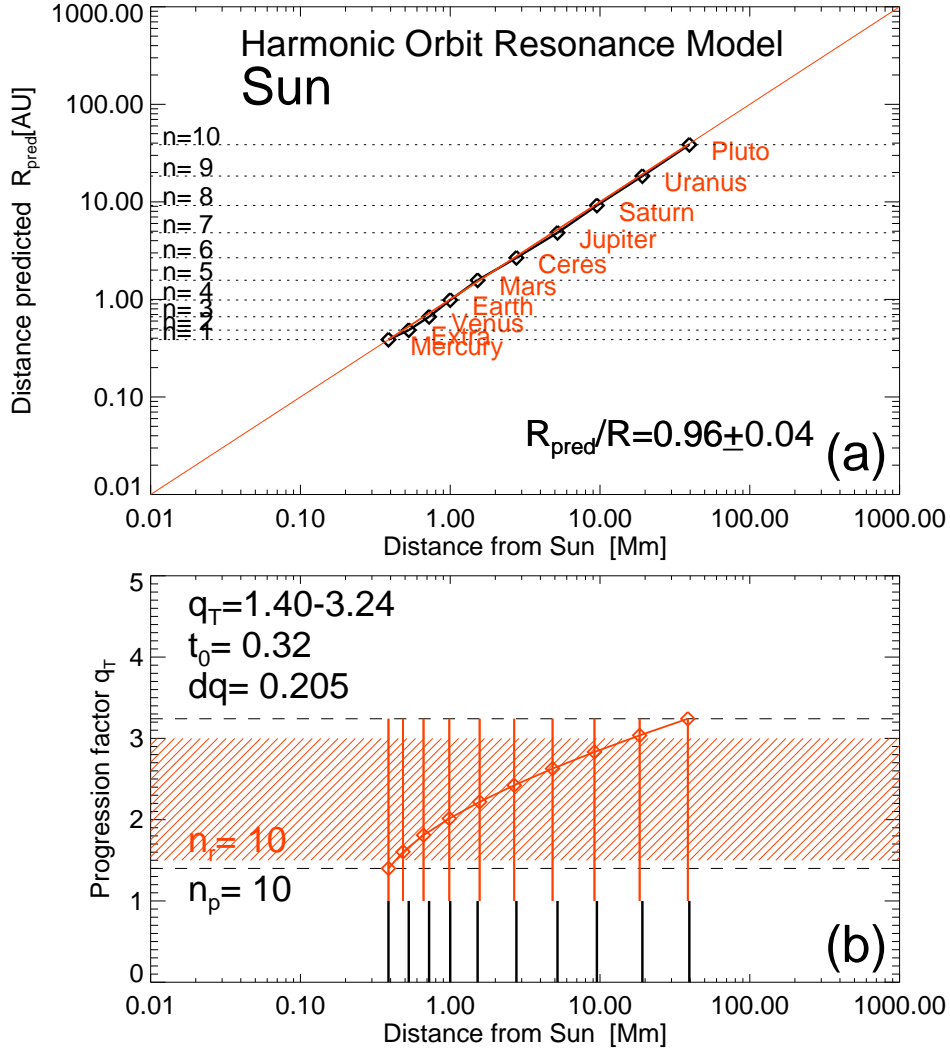


Fig. 5.— The distances of the planets from the Sun calculated with a harmonic orbit resonance model (a), for which the progression factor increases linearly with the orbit time,  $dq = 0.205$  (b). The observed distances are indicated with black tick marks, and the best-fit values with red lines and tickmarks. The zone between the minimum and maximum progression factor is indicated with dashed lines  $q_T = 1.40 - 3.24$ , and the theoretically predicted range  $q_T = 1.5 - 3.0$  with a red hatched area. In this model two planets are modified: an extra planet between Mercury and Venus is inserted, and the planet Neptune is eliminated.

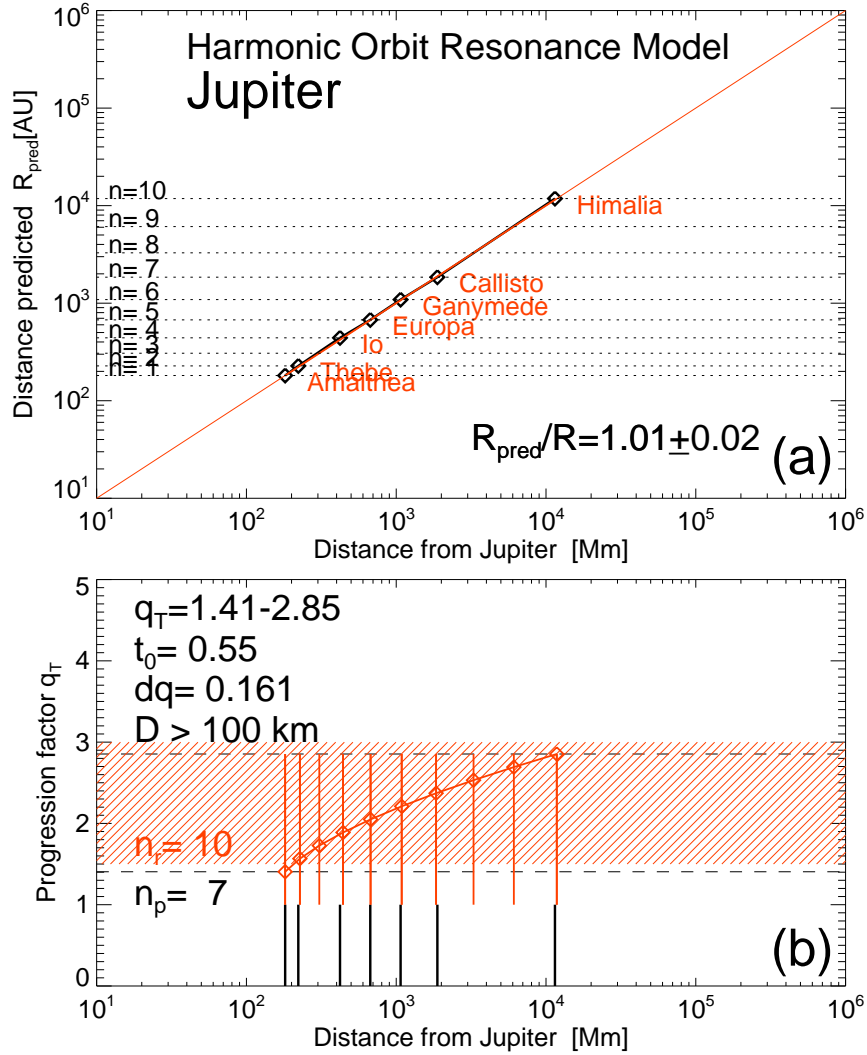


Fig. 6.— The distances of the seven largest ( $D > 100 \text{ km}$ ) moons from Jupiter are calculated with a harmonic orbit resonance model (a), for which the progression factor increases linearly with the orbit time (b). Representation otherwise similar to Fig. 5. Note that  $n = 10$  resonant zones fit  $n_p = 7$  observed moon distances.

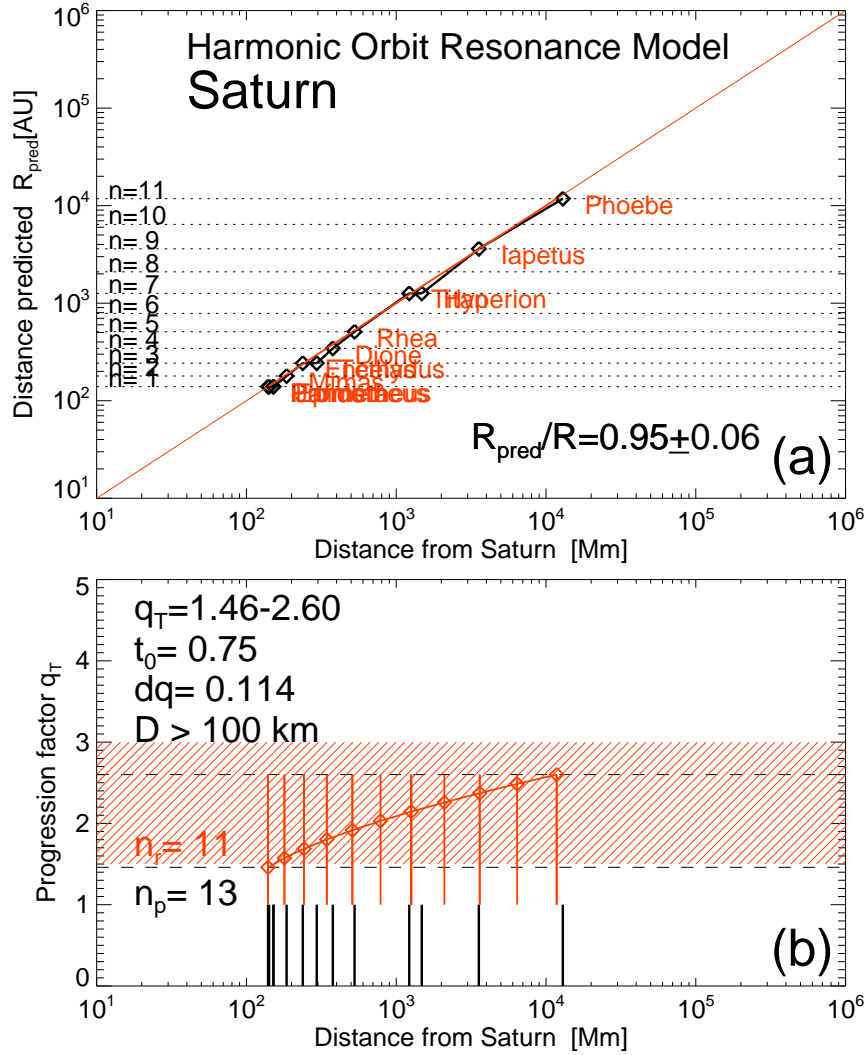


Fig. 7.— The distances of the 11 largest ( $D > 100 \text{ km}$ ) moons from Saturn are calculated with a harmonic orbit resonance model (a), for which the progression factor increases linearly with the orbit time (b). Representation otherwise similar to Fig. 5. Note that  $n = 13$  resonant zones fit  $n = 11$  observed moon distances.

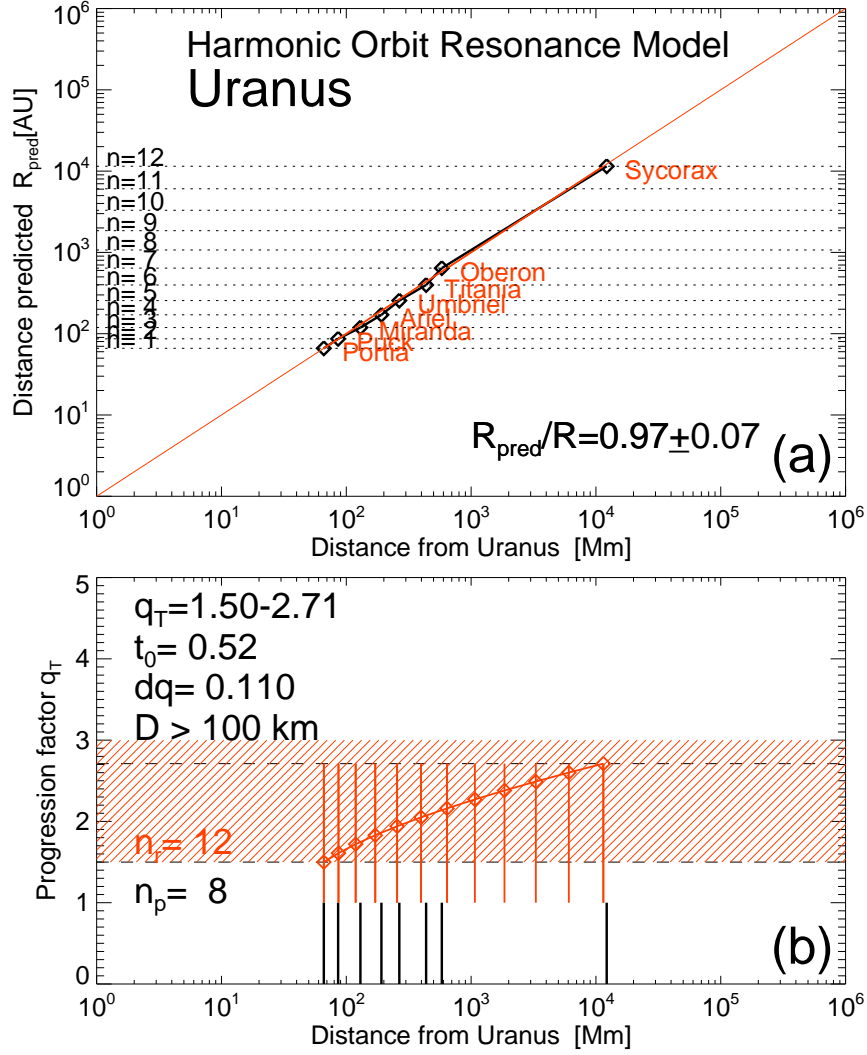


Fig. 8.— The distances of the eight largest ( $D > 100 \text{ km}$ ) moons from Uranus are calculated with a harmonic orbit resonance model (a), for which the progression factor increases linearly with the orbit time (b). Representation otherwise similar to Fig. 5. Note that  $n = 12$  resonant zones fit  $n = 8$  observed moon distances.

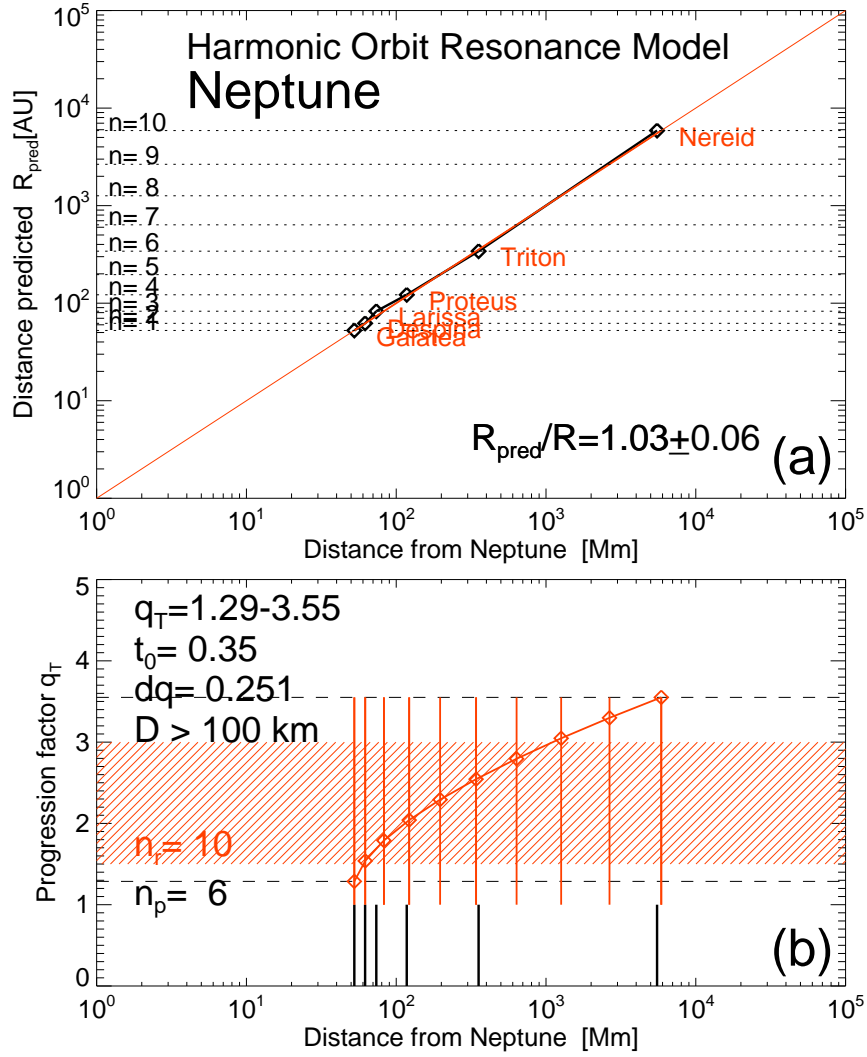


Fig. 9.— The distances of the six largest ( $D > 100 \text{ km}$ ) moons from Neptune are calculated with a harmonic orbit resonance model (a), for which the progression factor increases linearly with the orbit time (b). Representation otherwise similar to Fig. 5. Note that  $n = 10$  resonant zones fit  $n = 6$  observed moon distances.

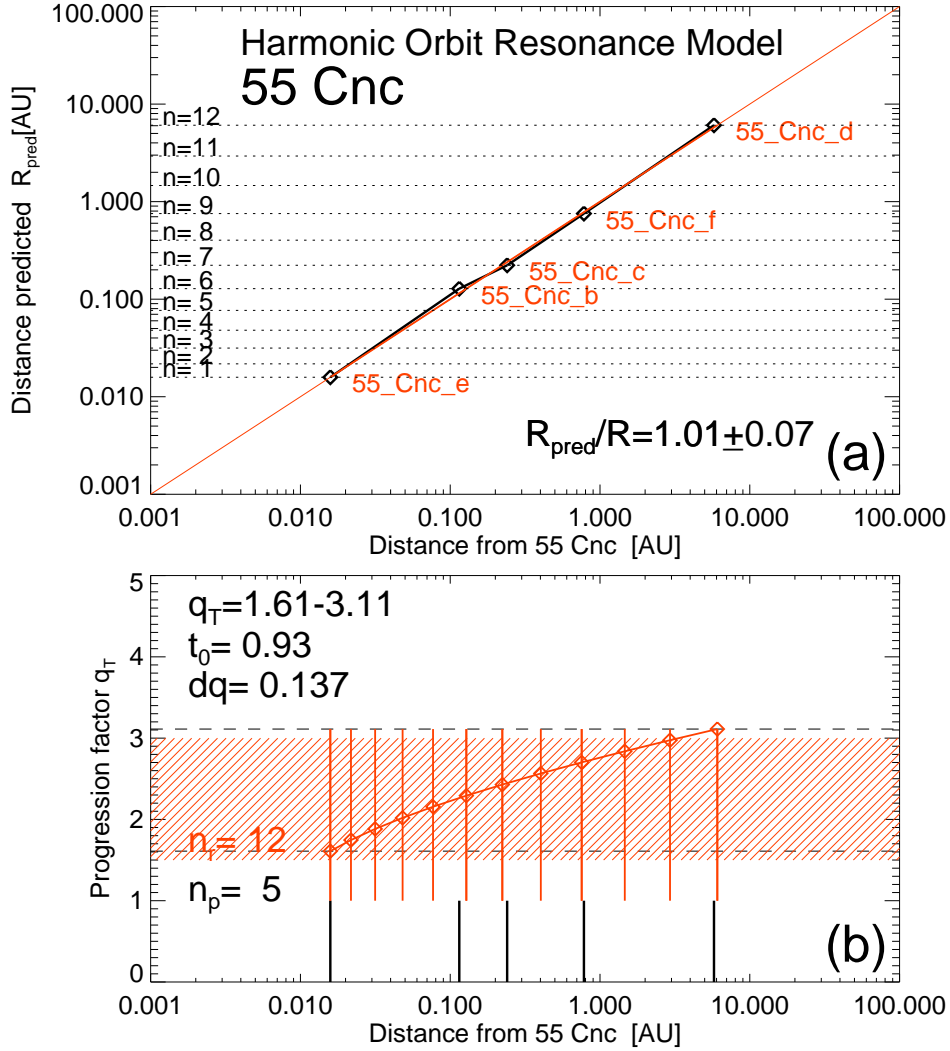


Fig. 10.— The distances of 5 exo-planets from their central star 55 Cnc are calculated with a harmonic orbit resonance model (a), for which the progression factor increases linearly with the orbit time (b). Representation otherwise similar to Fig. 5. Note that  $n = 12$  resonant zones fit  $n = 5$  observed exo-planet distances.

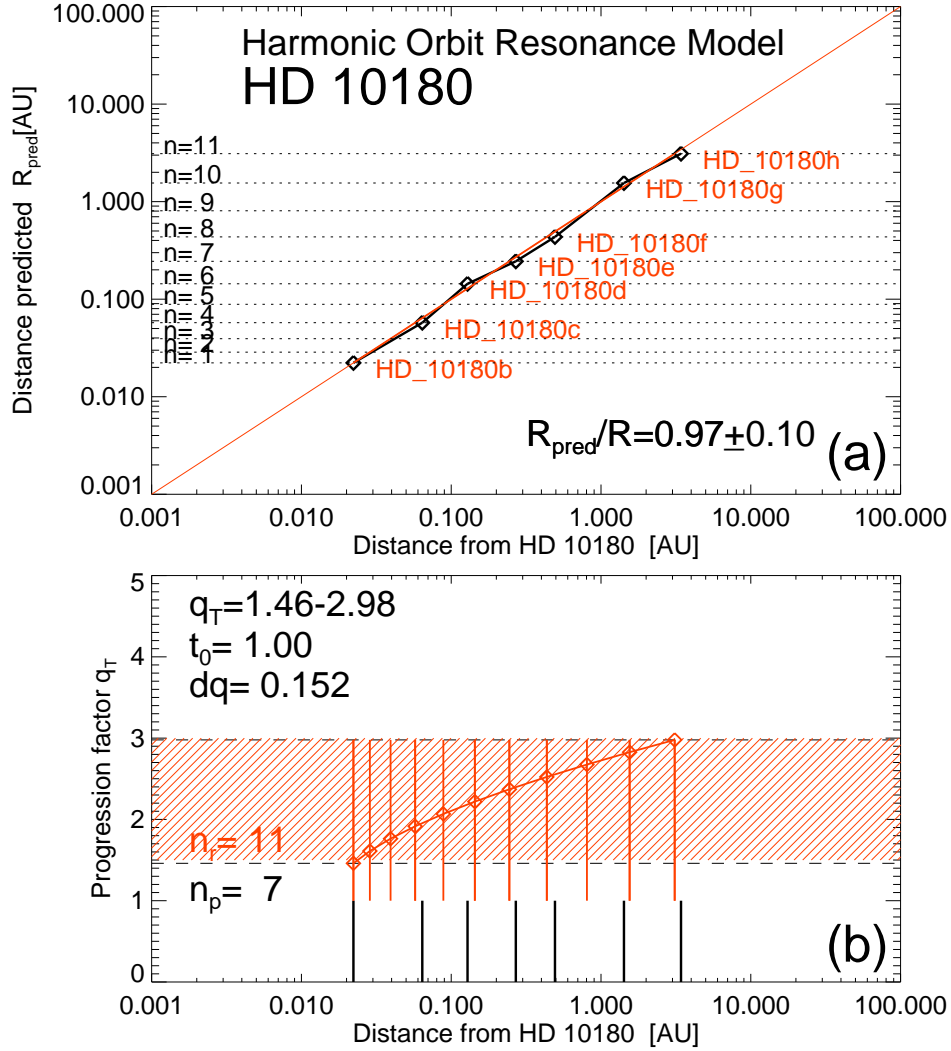


Fig. 11.— The distances of 7 exo-planets from their central star HD 10180 are calculated with a harmonic orbit resonance model (a), for which the progression factor increases linearly with the orbit time (b). Representation otherwise similar to Fig. 5. Note that  $n = 11$  resonant zones fit  $n = 7$  observed exo-planet distances.

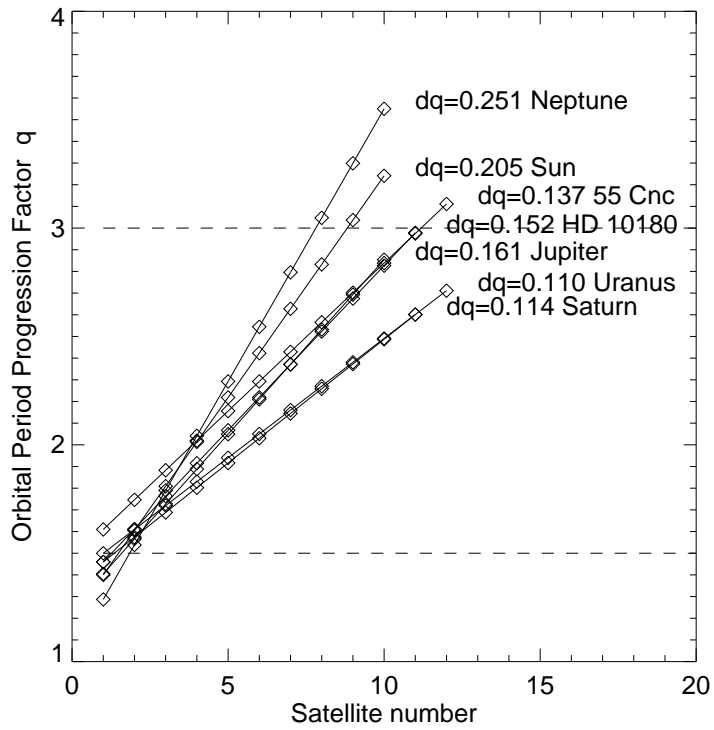


Fig. 12.— The progression factor  $q$  as a function of the satellite number, obtained from the best fits of the harmonic orbit resonance model to the data for the 8 data sets shown in Figs. 4-11.

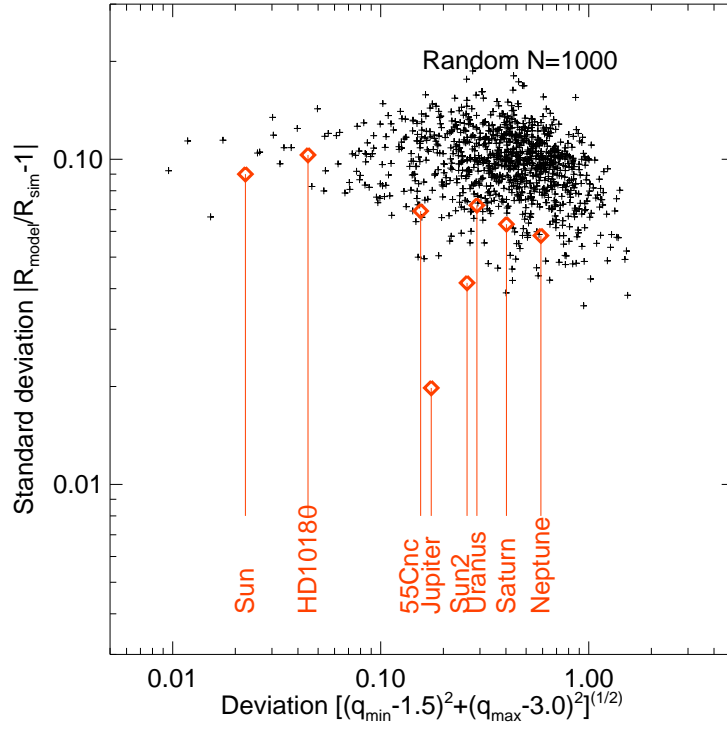


Fig. 13.— 1000 simulations (black crosses) of randomly distributed planet distances  $R$  are compared with the seven analyzed data sets (red diamonds). The quantity on the y-axis represents the standard deviation of the ratio of model distances  $R_{model}$  to the simulated distances  $R_{sim}$  for 1000 data sets with 10 planets each. The quantity on the x-axis represents the statistical deviation of the best-fit  $q$ -values (of the time period progression factor) from the theoretically predicted values  $q_{min} = 1.5$  and  $q_{max} = 3.0$ . Note that the results from the observed data sets are significantly different from those of the simulated random data sets.